

REPUBLIQUE ALGERIENNE DEMOCRATIQUE ET POPULAIRE

Université de Mohamed El-Bachir El-Ibrahimi - Bordj Bou Arreridj

Faculté des Sciences et de la technologie

Département d'électronique

Mémoire

Présenté pour obtenir

LE DIPLOME DE MASTER

FILIERE : Electronique

Spécialité : Industrie électronique

Par

- BELGOUMRI Younes
- MEDDAH Mohamed

Intitulé

study and optimization of the graded approach for boosting up the power conversion efficiency in solar cell-based perovskite □

Soutenu le : 04/07/2023

Devant le Jury composé de :

<i>Nom & Prénom</i>	<i>Grade</i>	<i>Qualité</i>	<i>Etablissement</i>
<i>M.DIB Lyes</i>	<i>MCB</i>	<i>Président</i>	<i>Univ-BBA</i>
<i>M.YOUSFI Abderrahim</i>	<i>MCB</i>	<i>Encadreur</i>	<i>Univ-BBA</i>
<i>M.DJEMOUAI Abdelouahab</i>	<i>MCB</i>	<i>Examineur</i>	<i>Univ-BBA</i>

Année Universitaire 2022/2023

Thanks

we would like to thank all the people who contributed to the success and who helped us during the writing of this dissertation. we would like to express our gratitude to our supervisor Dr. Yousfi Abderrahim, for his patience, availability and above all his wise advice, which helped to fuel our reflection.

Dedication

Many people stood by our side and provided us with support, without their encouragement, we would not have made it this far. Therefore, we would like to take this opportunity to dedicate this work:

To our Parents for their reassurance and prayers that helped us to stay on the track and reach this day.

To our siblings: Thank you for the many small things you did each day to push us through and for being supportive, our life is better because you are a part of it. You amaze and inspire me every day.

List of contents:

Thanks	
Dedication	
List of contents	
List of symbols and abbreviations	
List of figures	
List of tables	
Abstract	
General introduction	01
CHAPTER I: STATE OF THE ART	
Introduction	03
I.1 History:	03
I.2 Photovoltaic effect	04
I.3 Solar energy:	04
I.4 Solar spectrum:	04
I.5 Photovoltaic solar cell working principle:	05
I.6 Modeling of the photovoltaic cell:	06
I.7 Solar cell technologies:	07
I.7.1 First generation: Crystalline silicon (mono and poly):	07
I.7.2 Second generation: CdTe, CIS/ CIGS, amorphous Si and microcrystalline	07
I.7.3 Third Generation Photo-Electro-Chemical Technologies (Dye Sensitized	08
Cell, Organic PV and perovskite):	
I.8 Perovskite solar cells:	08
I.8.1 History of perovskite solar cells	08
I.8.2 Perovskite:	09
I.9 Perovskite solar cells architecture	10
I.10 Optoelectronic properties	11
I.10.1 Optical properties	12
I.10.2 Electronic properties.	12
I.11 Working principle of solar cells based on perovskite:	13
I.12 Transport materials	13
I.12.1 Electron transport layers	14
I.12.2 Hole transport layers	14

I.13 Photovoltaic cells Parameters.	14
I.13.1 Short-circuit current (J_{sc}).	15
I.13.2 Open-circuit voltage (V_{oc}).	15
I.13.3 Fill factor (FF).	15
I.13.4 Power conversion efficiency (PCE).	16
I.14. Advantages and disadvantages of photovoltaic energy.	16
I.14.1. Advantages.	16
I.14.2. Disadvantages.	16
Conclusion.	17

CHAPTER II: SCAPS-1D

Introduction	19
II.1 Software manipulation	20
II-2 Basic notion:	21
II.2.1 Simulation and Execution conditions:	21
II.2.2 Lighting condition:	22
II.2.3 Calculation's type and parameters:	22
II.2.4 Calculation and results:	22
II.2.5 Define the problem	23
II.3 The J-V curves:	24
II.4 Solar cell editing configuration:	24
II.4.1 Definition of layers:	25
II.4.2 Contacts:	28
Conclusion	29

CHAPTER III: RESULTS AND DISCUSSION

Introduction	31
III.1 Structure of the studied cell	31
III.1.1 Parameters of the studied perovskite cell:	32
III.2 ETLs effect on the solar cell performance	33
III.2.1 Thickness effect	33
III.2.2 Doping effect	34
III.3 Perovskite effect on the solar cell performance	35
III.3.1 Thickness effect of first perovskite layer ($CsSn_{0.5}Ge_{0.5}I_3$)	35
III.3.2 Doping effect of first perovskite layer ($CsSn_{0.5}Ge_{0.5}I_3$)	36
III.3.3 Thickness effect of second perovskite layer ($CsSnCl_3$)	36

III.3.4 Doping effect of second perovskite layer (CsSnCl ₃)	37
III.3.5 Thickness effect of third perovskite layer (CsSnCl ₃)	37
III.3.6 Doping effect of third perovskite layer (CsSnCl ₃)	38
III.4 HTL effect on the solar cell performance:	39
III.4.1 Thickness effect	39
III.4.2 Doping effect:	39
III.5 BSF effect on the solar cell performance	40
III.5.1 Thickness effect	40
III.5.2 Doping effect	41
Conclusion	42
General Conclusion	43
	45

List of symbols and abbreviations:

Si : Silicon.

PV : Photovoltaic.

UV : Ultraviolet

IR : Infrared.

AM : Air Mass.

J_{PH} : Photo - Current.

R_s: Series Resistance.

R_{sh} : Shunt Resistance

C-Si : Crystalline Silicon.

PECVD: Plasma Enhanced Chemical Vapor Deposition.

CdTe : Cadmium Telluride.

CIGS : Copper Indium Gallium Selenide.

OPV :Organic Photovoltaics Cells.

DSSCS : Dye-Sensitized Solar Cells.

PSCS : perovskite solar cells.

ABX₃ : Structure of generic a perovskite crystal.

EV: Electron Voltage.

λ : Wavelength.

ETL : Electron Transport Layer.

HTL : Hole Transport Layer.

HOMO : Highest occupied molecular orbital.

J-V : characteristic current-voltage.

J_{sc} : short-circuit current.

V_{oc} : Open circuit voltage.

FF : Fill Factor.

PCE : Power Conversion Efficiency.

P_{max} : Maximum Power.

P_i : Incident light power.

SCAPS : Capacitance Simulator One Dimension Plumb.

χ : Electron Affinity.

μ_n : electrons mobility.

μ_p : holes mobility.

N_A : Acceptor type doping density.

N_D : Donor type doping density

SRH : Shockley-Read-Hall.

List of figures:

Figure	page
CHAPTER I	
Figure I.1 Illustration of the photovoltaic effect	04
Figure I.2 Spectral distribution of solar radiation	05
Figure I.3 Photovoltaic solar cell working principle	06
Figure I.4 Equivalent electric circuit of the solar cell	06
Figure I.5 Photovoltaic solar cells evolution	07
Figure I.6 Solar cells efficiency Evolution versus years	09
Figure I.7: Perovskite Hybrid structure	10
Figure I.8: Most four architectures used in perovskite solar cells, (a) mesoporous, (b) cover layer, (c) n-i-p planar and (d) p-i-n planar	11
Figure I.9 Absorption coefficient functions of wavelength for different solar cell materials	12
Figure I.10: Operating Mechanism of a typical perovskite	13
CHAPTER II	
Figure.II.1: Main interface of SCAPS-1D.	15
Figure II.2: Working points	21
Figure II.3: Energy band panel	22
Figure II.4: Define the problem	23
Figure II.5: Panel of simulation results of the Illuminated J-V curve.	23
Figure II.6: Definition of layers in SCAPS	24
Figure II.7: Added layer properties	25
Figure II.8: Properties of defined doping	26
Figure II.9: Absorption model	27
Figure II.10: Recombination mode	27
Figure II.10 Recombination types definition.	28
Figure II.11: Contact properties panel.	29

CHAPTER III

Figure III.1: Structure of the suggested solar cell-based perovskite	32
Figure III.2: Thickness effect of ETL layer on performance solar cell	33
Figure III.3: Doping effect of ETL layer on performance solar cell	34
Figure III.4: Thickness effect of first perovskite layer on performance solar cell	35
Figure III.5: Doping effect of first perovskite layer on performance solar cell	36
Figure III.6: Thickness effect of second perovskite layer on performance solar cell	36
Figure III.7: Doping effect of second perovskite layer on performance solar cell	37
Figure III.8: Thickness effect of third perovskite layer on performance solar cell	38
Figure III.9: Doping effect of third perovskite layer on performance solar cell	38
Figure III.10: Thickness effect of HTL layer on performance solar cell	39
Figure III.11: Doping effect of HTL layer on performance solar cell	40
Figure III.12: Thickness effect of BSF layer on performance solar cell	41
Figure III.13: Doping effect of BSF layer on performance solar cell	41

List of tables:

Table	page
CHAPTER III	
Table III.1 Properties of the different layers of the proposed structure.	32
Table III.2 ETL Parametres for the suggested model	32
Table III.3 HTL Parametres for the suggested model	32
Table III.4 Comparison between the conventional and the suggested model	43

abstract

In general context of the diversified utilization of natural resources, the reference to renewable energy, especially solar photovoltaic energy, is becoming tremendous. Therefore, the development of a new photovoltaic generation of solar cell-based perovskite looks promising. In fact, the performance of this letter exceeded 30%. In this modeling via simulation, we use SCAPS-1D simulator to study the suggested structure of solar cell-based perovskite, the impact of different inputs like geometrical, optical and physical parameters on the output performance. We were particularly interested to study the influence of thickness and doping of all layers containing the solar cell such as ETL, absorber and HTL.

Résumé

Dans un contexte général de l'utilisation diversifiée des ressources naturelles, la référence aux énergies renouvelables, en particulier l'énergie solaire photovoltaïque, devient incontournable. Par conséquent, le développement d'une nouvelle génération photovoltaïque des cellules solaires à base de pérovskite semble prometteur. En fait, la performance de cette dernière a dépassé les 30 %. Dans cette modélisation par simulation, nous utilisons le simulateur SCAPS-1D pour étudier la structure suggérée de la cellule solaire à base de pérovskite, l'impact de différentes entrées telles que les paramètres géométriques, optiques et physiques sur les performances de sortie. Nous nous sommes particulièrement intéressés à étudier l'influence de l'épaisseur et du dopage de toutes les couches contenant la cellule solaire telles que l'ETL, l'absorbeur et le HTL.

ملخص:

في السياق العام للاستخدام المتنوع للموارد الطبيعية، تصبح الإشارة إلى الطاقات المتجددة، ولا سيما الطاقة الشمسية الكهروضوئية، أمرًا لا مفر منه. لذلك، فإن تطوير جيل جديد من الخلايا الشمسية القائمة على البيروفسكايت يبدو واعدًا. والواقع أن أداء الأخير تجاوز 30٪. في نمذجة المحاكاة هذه، نستخدم محاكي SCAPS-1D لدراسة الهيكل المقترح للخلية الشمسية القائمة على البيروفسكايت، وتأثير المدخلات المختلفة مثل المعلمات الهندسية والبصرية والفيزيائية على أداء المخرجات. لقد طلبنا من أنفسنا بشكل خاص فحص تأثير سمك والمنشطات لجميع الطبقات التي تحتوي على الخلية الشمسية مثل ETL والممتص وHTL.

GENERAL

INTRODUCTION

General Introduction

With the tremendous progress of industry, our lives have become more convenient, but at the same time, energy crisis and climate change have also become issues that we cannot ignore. Thus, advancing renewable energy is an important topic for today and for the future. Solar energy as one of the renewable resources is promising for future energy supplies. This provides a motivation for scientists to work on the development of solar cells.

Solar energy considered as one of the best alternative clean energies. She might be operated using two main techniques: thermal or voltaic. Solar energy photovoltaic is electrical energy resulting from a direct conversion of radiation solar.

Solar energy resources are not inexhaustible and non-polluting energy; it could be installed in any region and its use requires little regular maintenance. It's an applicable technique in several sectors, it has the following advantages [1]:

- Cost: the energy will become almost free once the price of the equipment is amortized.
- Autonomy: with energy storage technology, the photovoltaic system constitutes an autonomous network.
- Quantity: photovoltaic energy is unlimited.

Photovoltaic solar energy is a technique that effectively responds to the challenges energy and environmental, and represents a realistic approach that promotes the sustainable development. Photovoltaic technology is based on certain semiconductor materials. Currently, it is silicon-based photovoltaic technologies which dominate the photovoltaic market. Solar cells are currently the subject of much research with the aim of achieve the best ratio between energy efficiency and cost price. Researchers turned to simulation as a means to low cost. The object of this dissertation is study and optimization of the graded approach for boosting up the power conversion efficiency in solar cell-based. This thesis is composed of three chapters, The first chapter, is about general notions on photovoltaic energy. The second chapter, we will introduce the SCAPS-1D software simulator. And we finish by, results and discussion of the suggested model of solar cell based-perovskite then conclusion.

CHAPTER I

STATE OF THE ART

STATE OF THE ART

Introduction:

Today, photovoltaic energy is one of the renewable energy technologies which plays a major role in the future of electricity production. To reach industrial demonstration, photovoltaic technology must take into account the following three main factors: efficiency, stability and low cost, at first, we will describe some notions of the source of photovoltaic energy, then we will talk about different photovoltaic cell technologies, exactly perovskite with their characteristics and we finish with advantages and disadvantages of photovoltaic energy.

I.1 History:

photovoltaic effect was discovered by physicist Alexandre Edmond Becquerel. He has experimented with this phenomenon by illuminating platinum electrodes covered with chloride or of silver bromide (AgCl-AgBr) in a liquid, he observed the presence of a photo-current [2].

Smith and Adam were the first to write reports on the photoconductivity of selenium material in 1873 and 1876 respectively. In 1905, Albert Einstein explained the photoelectric phenomenon which earned him the Nobel Prize of physics in 1921. Anthracene (C₁₄H₁₀) was the first organic compound in which the photoconductivity was observed respectively by Pochettino in 1906 and by Volmer in 1913[3]. In 1954, Bell laboratory researchers developed for the first time an inorganic solar cell with an efficiency of 4% [4]. In 1958, Hoffman Electronics made photovoltaic cells with an efficiency of 9%, then 2 years later, it produced cells efficient photovoltaic systems by 14% [1]. At the end of the fifties, the photoreceptors based on organic compounds are widely used in systems imagery. Also, it was discovered in the 1960s that certain common dyes such as methylene blue have semiconductor properties [3]. Moreover, the photovoltaic effect has been observed in several biological molecules such as carotenes, chlorophylls and porphyrins [2]. Interest scientific and commercial potential have multiplied research in the field of photovoltaics. The power conversion efficiency of solar cells is improving over the years until the efficiency of crystalline solar cells reaches 24%. Today the Silicon (Si)-based solar cells dominate the photovoltaic cell market with their greater efficiency and great stability. The development which has known the silicon-based photovoltaic technology has greatly reduced the cost of production and the global PV market has increased considerably over the past 20 years. In order to reduce costs and increase efficiency, solar cell based-perovskite is important and necessary in order to achieve both conditions due to its low temperature technology, low cost, flexible devices and different raw materials. Both organic and inorganic photovoltaics are still in the laboratory research and development stage. Despite

the impressive progress, this challenge mainly depends on developing a lower cost process and better conversion efficiency.

I.2 Photovoltaic effect

Photovoltaic effect is a phenomenon that allows the conversion of light energy into electricity, through a semiconductor material responsible for transporting electric charges as shown in Figure I.1.

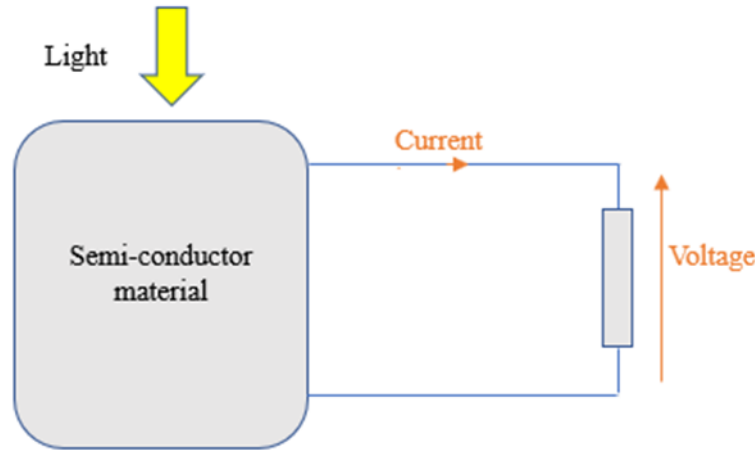


Figure I.1 Illustration of the photovoltaic effect [3]

I.3 Solar energy:

Solar energy emits what is called solar radiation, considered the best combined energy source on the planet. The amount of energy emitted from the sun that the earth would absorb for an hour could be enough to cover the world's energy needs. It releases a huge amount of radiant energy as the photovoltaic cell converts it into electrical energy based on the physical phenomenon called the photoelectric effect, which consists of producing an electromotive force when the cell is exposed to light. The voltage generated by the solar cell may vary depending on the material used to manufacture the solar cell.

I.4 Solar spectrum:

The sun is considered a black body, it absorbs all electromagnetic waves radiation and consequently emits radiation of all energies including in the visible area. The maximum intensity of the solar spectrum is located at 500 nm as presented in figure I.2. The sun radiates into space in ultraviolet (UV), visible and infrared (IR) light, these emissions span the entire

electromagnetic spectrum. However, the atmosphere plays the role of filter to protect the earth from dangerous emissions [5]. Several factors influence the solar spectrum [6]:

- a) Raleigh Broadcast responsible for the blue color of the sky;
- b) Absorption by oxygen (O₂), nitrogen (N₂) and the O₃ zone;
- c) Aerosol diffusion;
- d) Refraction due to variations in refractive index with temperature and pressure.

The intensity of solar radiation is reduced on earth because of the losses caused by atmospheric absorption, this loss of energy is called the air mass (AM), there designation of AM0 corresponds to the mass of air which arrives above the atmosphere, however AM1.5 corresponds to a solar spectrum under an angle of inclination of 48.2° by relative to the zenith, equivalent to a power energy flow of 1000 W/m². By virtue of lamps associated with lenses, the solar spectrum on the surface of the earth is simulated in the laboratory [7], which makes it possible to reproduce the AM1.5 spectrum used as an industry standard in the characterization of solar cells.

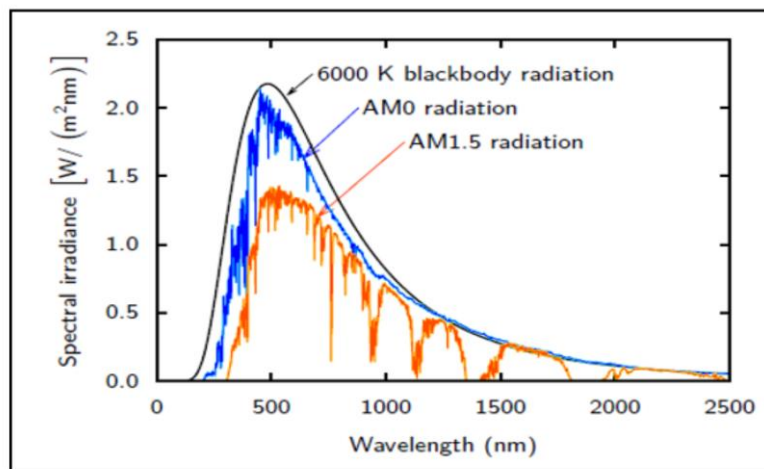


Figure I.2 Spectral distribution of solar radiation [8]

I.5 Photovoltaic solar cell working principle:

Solar cell is one of the semiconductor components that convert light into electrical energy. The aforementioned phenomenon, the optical effect, comes from the potential difference resulting from the generation of charge carriers by excitation light near the junction. A solar cell is a *p-n* junction working under illumination. When we make in adjacency the two layers *n* and *p*, that leads to flow some holes from *n* to *p* layer and electrons from *p* to *n* as shown in

figure I.3, the $p-n$ junction operation depends on the absorption of the solar luminous flux. As for the effect photoelectric used in solar cells, it can convert energy directly from sunlight into electricity by generating and transmitting positive and negative electrical charges in a semiconductor material under the influence of light.

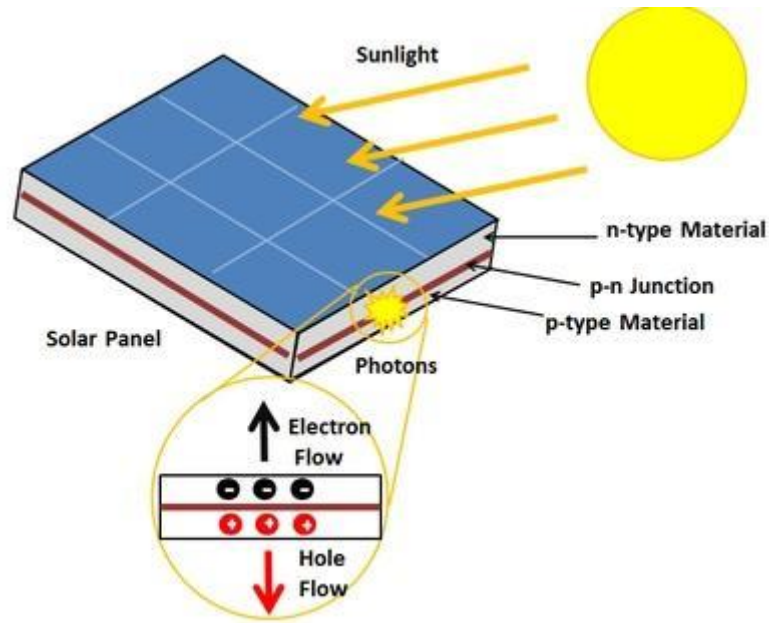


Figure I.3 Photovoltaic solar cell working principle. [9]

I.6 Modeling of the photovoltaic cell:

The corresponding figure I.4 is the equivalent electric circuit of a photovoltaic solar cell exposed to the sun, where we see the I_{ph} generator connected in parallel with the diode, The series resistance R_s constitutes the resistance of the material and the ohmic contacts when the cell is connected to an external circuit, while the shunt resistance R_{sh} models the resistance due to recombination of the conductors at each donor interface and also at the interface of the electrodes.

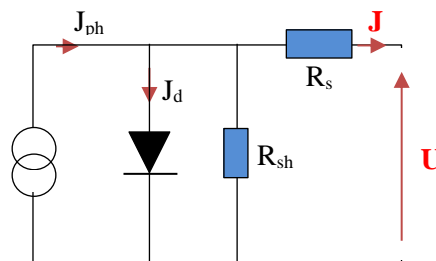


Figure I.4 Equivalent electric circuit of the solar cell [10]

I.7 Solar cell technologies:

Several technologies are used in the design of a photovoltaic solar cell in order to implement the photovoltaic effect, many of them are still in the phase of experimentation and development. Photovoltaic cells are made from many semiconductor materials which can be inorganic, organic or hybrid. At present there is three generations of photovoltaic cells technologies as presented in figure I.5:

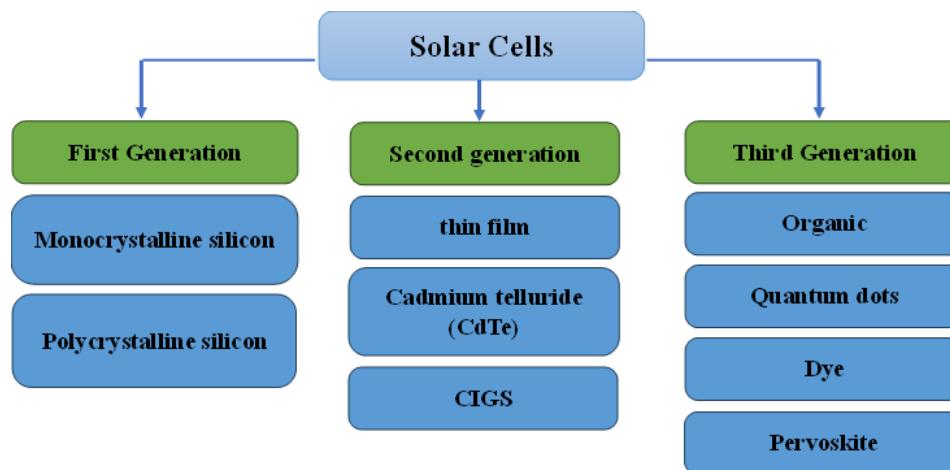


Figure I.5 Photovoltaic solar cells evolution [11].

I.7.1 First generation: Crystalline silicon (mono and poly):

The first-generation of photovoltaic cells technology is the conventional PV system that utilizes crystalline silicon (c-Si), whether in single-crystalline or multi-crystalline forms. They accounted for about 95% of the total PV production in 2021 [12]. Although they have high efficiency and occupy a large part of the PV market, they have disadvantages of high manufacturing costs. Crystalline Si has indirect bandgap which results in a relatively low absorption coefficient (100 cm^{-1}). A typical thickness of $250 \mu\text{m}$ is needed for Si wafer to have a sufficient absorption of light [13].

I.7.2 Second generation: CdTe, CIS/ CIGS, amorphous silicon and microcrystalline

This generation of cell is based on the deposition of semiconductor materials in layers thin (thin film). These materials are deposited by processes such as PECVD (Plasma Enhanced Chemical Vapor Deposition) on a substrate. The thickness layer varies between a few nanometers to tens of micrometers. These technologies which were initially expensive ones were reserved for space applications and advanced technologies. With the increase of production volumes, the cost price of these technologies has fallen to become competitive with the technologies of first-generation crystals. Among the thin-film technologies that are used

industrially (production of mass), we distinguish: -CdTe: Cadmium Telluride (Cadmium telluride), CIS / CIGS: Copper Indium Gallium Selenide, Thin film silicon: amorphous silicon α -Si and microcrystalline. Note that cadmium telluride is a heavy metal alloy and very toxic.

I.7.3 Third Generation Photo-Electro-Chemical Technologies (Dye Sensitized Cell, Organic PV and perovskite):

Third-generation PV technologies are developed for the purpose of pursuing high conversion efficiency performance, or even exceed the Schokley-Quiser limit, or the development of innovative architectures at low prices. They include cells under concentration, multi-junction, organic photovoltaic cells (OPV), solar dye cells (DSSCS) and Perovskite solar cells (PSCS)[14].

I.8 Perovskite solar cells:

I.8.1 History of perovskite solar cells

Perovskite solar cells it was discovered by the Russian mineralogist Lev Alexeïevich Perovski (1792– 1856). Among thin-film solar cell technologies, metal halide perovskite solar cells have emerged recently. Within a very short time, it was found that it constitutes a competitive new category towards the next generation of highly efficient and cost-effective photovoltaic systems. The technology uses very cheap raw materials, and the curing is favorably characterized by low cost, low deposition temperature, and proportional to flexible substrates and large surface areas. Perovskite solar cells have shown a remarkable progress in recent years with rapid increases in efficiency, from reports of 3% in 2009 to over 25% today as shown in figure I.6.

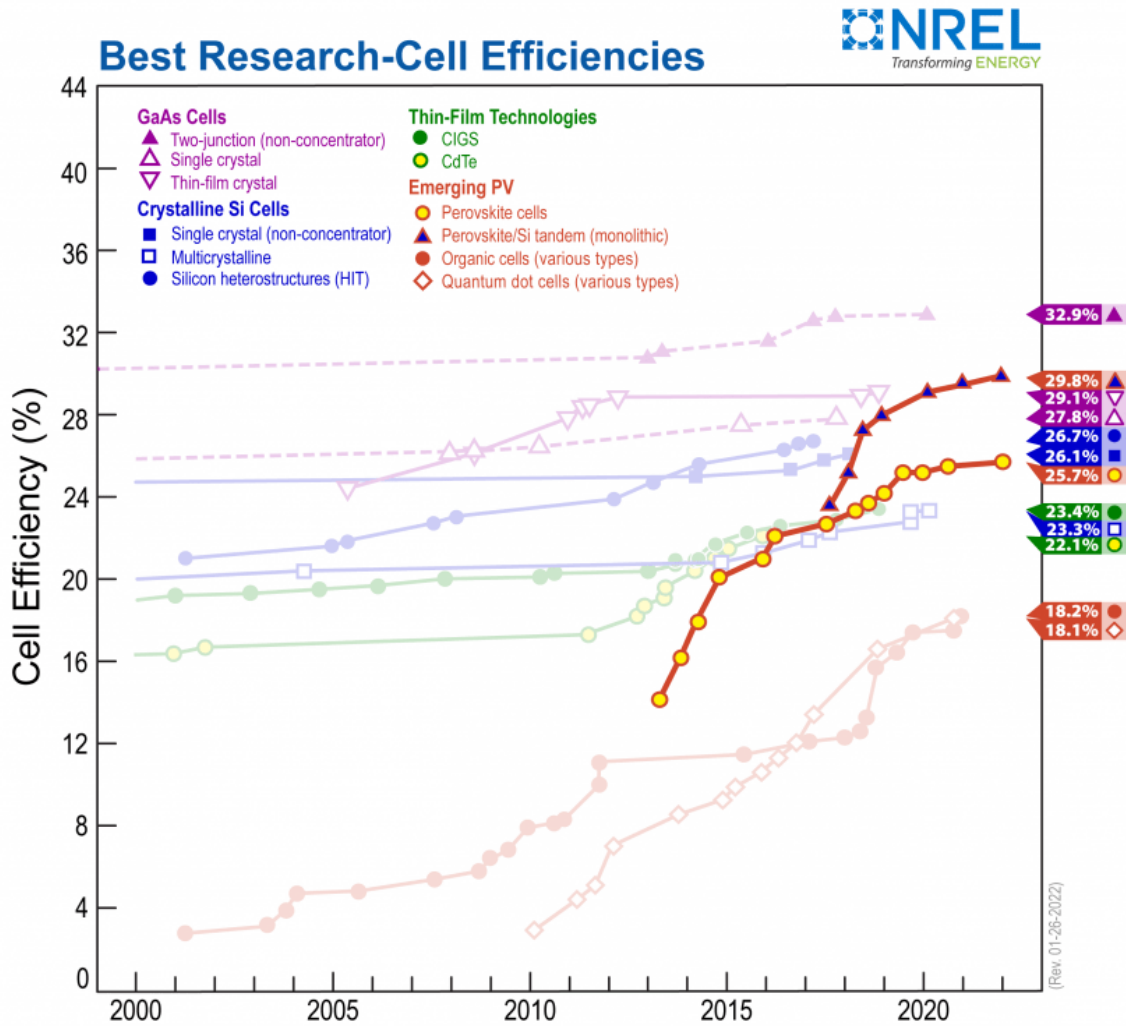


Figure I.6 Solar cells efficiency Evolution versus years [15]

I.8.2 Perovskite:

Halide perovskites are a family of materials that have shown potential for high performance and low production costs in solar cells. The name “perovskite” comes from the nickname for their crystal structure, although other types of non-halide perovskites (such as oxides and nitrides) are utilized in other energy technologies, such as fuel cells and catalysts a metal halide perovskite is the name for a class of materials with a general structure ABX_3 as illustrated in figure I.7, in which the hexagonal metal cation B occupies an octahedral center sharing halide x atoms on its vertices. Another additional cation, A, is located in the spaces between adjacent octahedrons. the metal halide perovskite as a whole must be electrically neutral so cation A is monovalent, cation B is divalent, and anion (halide), X is monovalent. with elements A, B and X can be [16].

A: cation (Cs^+ , Rb^+ , MA^+ , FA^+ , ...),

B: cation (Pb^{2+} , Sn^{2+} , Ge^{2+} , ...),

X: anion (halides (I^- , Br^- , Cl^- , ...))

The most widely used perovskite is the methyl-ammonium lead triiodide compound $\text{CH}_3\text{NH}_3\text{PbI}_3$ (MAPbI_3) which is deposited as an autoclave, its energy in the range of 1.55-1.6 eV, which corresponds to an absorption threshold at $\lambda = 550 \text{ nm}$. It allows total absorption of photons with energy higher than the forbidden range within one micrometer.

The excitons generated in perovskites easily dissociate into free electrons and holes only by thermal activation at room temperature, the lifetime of free carriers is good in the order of microseconds as well as sufficient kinetics in the range of $10\text{-}40 \text{ cm}^2/\text{V}\cdot\text{s}$.

The group of perovskite cells usually consists of a thin absorbing layer with a thickness from 300 nm to 400 nm sandwiched between holes and electron selective layers (HTL, ETL, respectively) adjacent to the contacts.

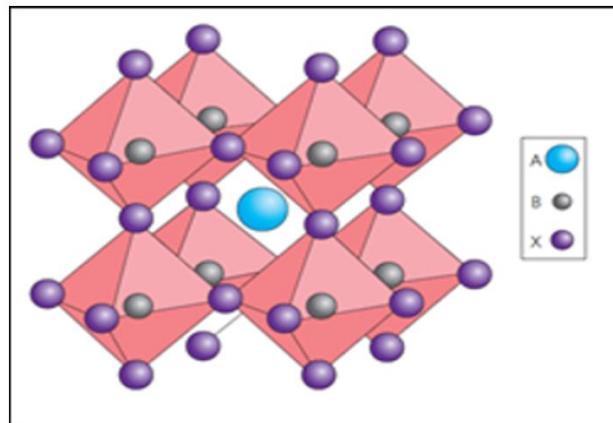


Figure I.7: Perovskite Hybrid structure [17].

I.9 Perovskite cells architecture:

There are four main architectures used in the design and manufacture of perovskite-based solar cells with different performances. These architectures are called mesoporous, cap layer, planar n-i-p and p-i-n planar, as shown in figure I.8. For modeling and simulation digital, it will be preferable to use the configuration of a film solar cell thin p-i-n or n-i-p planar heterojunction type.

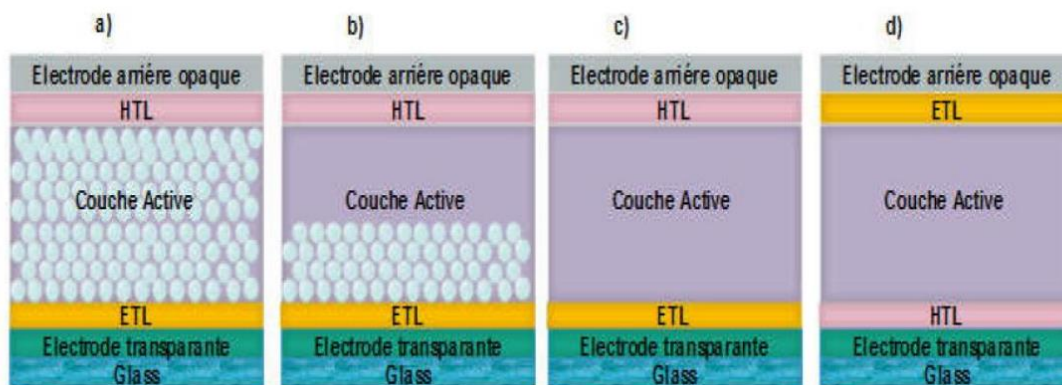


Figure I.8: Most four architectures used in perovskite solar cells, (a) mesoporous, (b) cover layer, (c) n-i-p planar and (d) p-i-n planar [18]

Figure I.8.a presents a mesoporous structure, in this architecture a compact electron transport layer (ETL) usually TiO_2 is deposited on a glass substrate and on the transparent electrode. This porous mesoscopic structure is then filled with the perovskite active layer on which the transport layer rests solid holes (HTL), and an opaque back contact (usually gold (Au)). In this configuration, the perovskite does not need the ETL/perovskite interface to separate the photo-generated excitons in free charges. The perovskite-based material is therefore capable of efficiently carrying ambipolar loads. For architecture mesoporous with covering layer, the thickness of the mesoscopic structure is significantly reduced and a capping-layer of pure perovskite is created on top figure I.8.b, by completely excluding the mesoporous structure, a planar n-i-p structure is formed without the need of high-temperature sintering step (Figure I.8.c). The planar p-in architecture is achieved by depositing the HTL layer on the transparent glass substrate covered by the electrode, perovskite layer is deposited, followed by the deposition of the ETL and an opaque rear contact (aluminum (Al) or silver (Ag)) (Figure I.8.d).

I.10 Optoelectronic properties

The interest shown in oxides of perovskite structure ABX_3 for more than four decades, results in the ease of changing the nature of the A and B cations present in the structure. As a result, this modification of the elements leads to a change in the properties of the material thus leaving the door open to all kinds of physical properties in function of the chemical and electronic nature of the two atoms A and B [19].

I.10.1 Optical properties

Perovskite has a direct bandgap material and therefore it has a high optical absorption force and a wider range to absorb enough solar energy to achieve high power conversion efficiency value [20]. From (figure I.9) it can be seen that at the visible wavelength the perovskite absorption coefficient is higher. So, the perovskite can absorb more photons. This great absorption, compared to that of crystalline silicon, makes it possible to reduce the thickness of perovskite layer to 500 nm for near absorption [21].

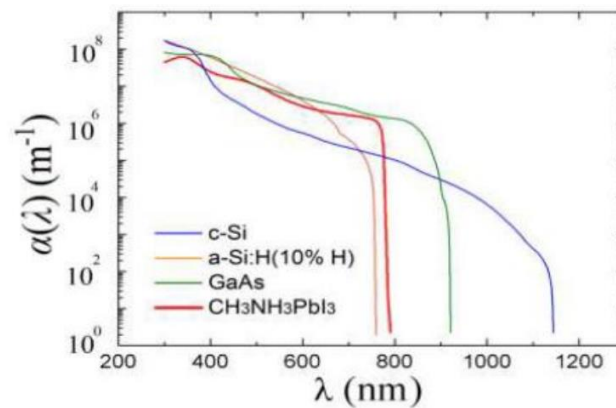


Figure I.9 Absorption coefficient functions of wavelength for different solar cell materials [22]

I.10.2 Electronic properties:

They are superconducting at relatively high temperatures, they transform mechanical pressure or heat into electricity (piezoelectricity), accelerate chemical reactions (catalysts) and suddenly change their electrical resistance when they are placed in a magnetic field (magnetoresistance), numerous electrochemical studies on the electrodes based on these oxides were carried out in an aqueous medium [23]. They have revealed an important electrocatalytic role in the electrode reaction at oxygen at room temperature. Perovskite becomes ionic and covalent, dual nature in electronic structures. The diffusion length of electrons and holes is an important characteristic in the field of photovoltaics since it will come into play in the choice of the thickness of the active layer. In the case of silicon, the diffusion length is a few hundred micrometers [24]. For perovskite, the diffusion lengths of carriers are much lower than those of silicon. Diffusion lengths of the order of 100 nm for holes and electrons were measured by photoluminescence on a layer of MAPI with a thickness of 180 nm, but up to 1 μm for thin layers of MAPI_{3-x}Cl_x with a thickness of 270 nm [25].

I.11 Working principle of solar cells based on perovskite:

In a perovskite cell, the active layer is sandwiched between a p-type layer, also called HTM (Hole Transport Material), and an n-type layer called ETL (Electron Transport Layer), thus creating a p-i-n configuration. The success of perovskite as a solar absorber widely depends on the long length of diffusion of charges and high mobilities of carriers in the medium. The working principle of perovskite solar cells after sunlight irradiates the light absorbing layer (perovskite layer), photons with energy greater than the forbidden band width are absorbed, the energy of the photon excites electrons that were originally bound around the nucleus, producing excitons (electron-hole pairs) as shown in (figure I.10). Due to the small exciton binding energy of perovskite materials, they can be separated into free carriers (electrons and holes) at room temperature. After the excitons are separated into electrons and holes, the holes enter the hole transport layer (HTL) from the perovskite material, electrons enter the electron transport layer (ETL) from the perovskite material and flow to the cathode and anode of the battery, respectively.

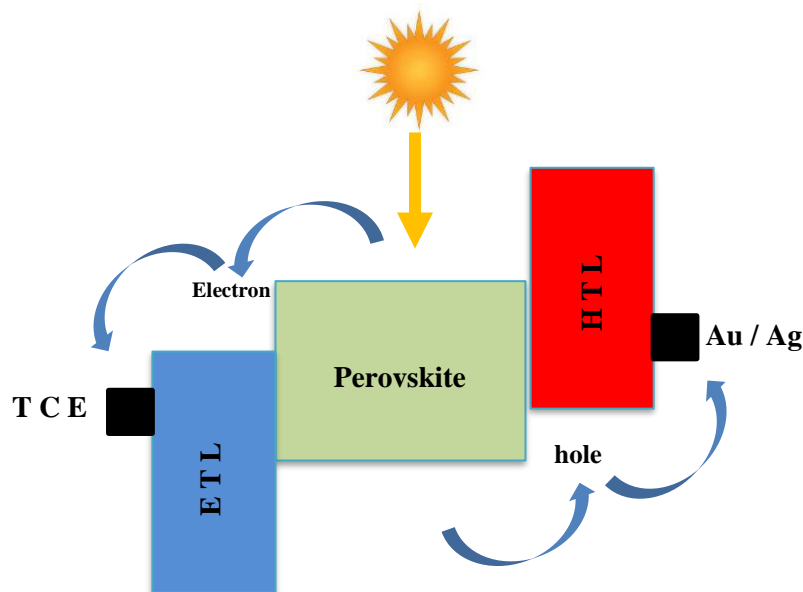


Figure I.10: Operating mechanism of a typical perovskite.[25]

I.12 Transport materials

In a perovskite solar cell, the ETL, HTL and perovskite layers are the path, that the photo-generated carriers must move before being collected. A good understanding of the effects of each of these layers on performance is essential for cell optimization.

I.12.1 Electron transport layers

Electron transport layer (ETL) is an n-type semiconductor layer, his role is to transport electrons from perovskite layer(absorber) to front contact. For a material to be used as an electron transport layer in perovskite solar cells, it must have high electron mobility and higher band gap [26]. That is why organic-inorganic materials are widely used in perovskite solar cells as electron transport layers. With high electron mobility, they can perform electron transmission efficiently.

I.12.2 Hole transport layers

Holes transport layer (HTL) is a p-type semiconductor layer, we use it to transport the holes from the perovskite layer to the back contact. The use of hole transport material (HTL) in solar cells based on perovskite is essential [27]. This layer presents an energy barrier physics between the anode and the perovskite layer which blocks the transfer of electrons to anode [28], it also improves hole transfer efficiency at the presence of a HTL layer [29]. For efficient hole extraction at the perovskite-HTL interface, the HTL layer must have:

- High mobility of the holes to reduce losses during transport holes to the collector contact.
- An ionization potential consistent with that of the perovskite (i.e. the orbital band maximum (HOMO) should be slightly above of the valence band of the perovskite layer in order to minimize losses by injection.
- High thermal stability and strong resistance to stress factors external degradation such as humidity and oxygen for a long-term sustainable PV operation.

I.13 Photovoltaic cells Parameters:

Solar cell usually characterized by the current-voltage characteristic J-V. The main parameter that are used to characterize the performance of solar cells are the short-circuit current density J_{SC} , the open circuit voltage V_{OC} , the fill factor FF, and conversion efficiency PCE.

These parameters are determined from the illuminated characteristic J-V as illustrated in figure I.11. The conversion efficiency PCE can be determined from these parameters.

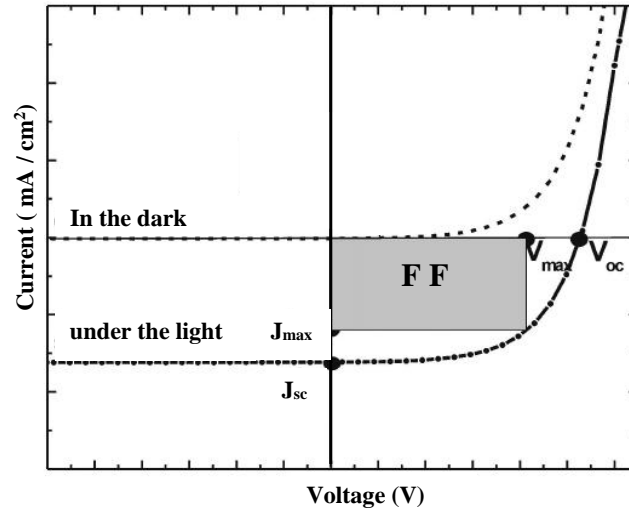


Figure I.11 Characteristics J-V [6]

I.13.1 Short-circuit current (J_{sc}):

Short-circuit current is the current that flows through the external circuit when the electrodes of the solar cell are short circuited. The short-circuit current of a solar cell depends on the incident photon flux on the solar cell, which is determined by the spectrum of the incident light.

$$J_{SC} = \frac{J_{ph}}{1 + \frac{R_s}{R_{sh}}} \dots\dots\dots I.1$$

I.13.2 Open-circuit voltage (V_{oc}):

The open-circuit voltage is the voltage at which no current flows through the external circuit, it is the maximum voltage that a solar cell can deliver. V_{OC} corresponds to the forward bias voltage, at which the dark current density compensates the photocurrent density. V_{OC} depends on the photo-generated current density and can be calculated from Eq. (I.2) assuming that the net current is zero,

$$V_{OC} = \frac{K_B T}{q} \ln \left(\frac{J_{ph}}{J_0} + 1 \right) \approx \frac{K_B T}{q} \ln \left(\frac{J_{ph}}{J_0} \right) \dots\dots\dots I.2$$

I.13.3 Fill factor (FF):

The fill factor is the ratio between the maximum power (P_{max} = J_{mpp} × V_{mpp}) generated by a solar cell and the product of V_{OC} with J_{SC} that is to say the ratio of the areas of the two rectangles gray and light, the fill factor is given by the expression I.3:

$$FF = \left(\frac{J_m \cdot V_m}{J_{sc} \cdot V_{oc}} \right) \dots \dots \dots I.3$$

I.13.4 Power conversion efficiency (PCE):

The power conversion efficiency PCE in a photovoltaic solar cell represents the ratio between the maximum power delivered by the PV cell and the forward power received as expressed to equation I.4

$$PCE = \left(\frac{P_m}{P_i} \right) = \frac{J_m \cdot V_m}{P_i} = \frac{J_{sc} \cdot V_{oc}}{P_i} * FF \dots \dots \dots I.4$$

P_i: incident light power,

P_m: the maximum power converted into electricity.

I.14. Advantages and disadvantages of photovoltaic energy:

1.14.1. Advantages:

High reliability; modules are guaranteed for 25 years by most manufacturers. It has no moving parts, which makes it particularly suitable to isolated regions. This is the reason for its use on spacecraft. The nature of modulator of the photovoltaic panels allows the simple and adaptable to various energy needs. Systems can be sized to power applications ranging from milliwatts to megawatts; Their operating costs are very weak given the discounted interviews, and they do not require fuel or transportation or highly specialized personnel. Photovoltaic technology has ecological qualities because the final product is non-polluting, silent, little waste.

1.14.2. Disadvantages:

The manufacture of the photovoltaic module is high technology and requires high-cost investments; occupation of space for large installations; the actual conversion efficiency of a module is low (the theoretical limit for a crystalline silicon cell is 28%); photovoltaic generators are not competitive with diesel generators only for low energy demands in isolated areas;

Finally, when the storage of electrical energy in chemical form (battery) is necessary, the cost of the photovoltaic generator is increased, reliability and performance of the system remain equivalent. However, provided that the battery and the components of associated regulations are wisely chosen.

Conclusion:

Although the efficiency of PSCs has increased to more than 20%, competitive with established photovoltaic technologies, such as silicon solar cells and thin-film solar cells, to take PSCs from intense laboratory research to commercialization Outdoors, there are still two main challenges: toxicity in lead perovskites and long-term stability. However, understanding the degradation mechanism of PSCs and the device architecture may provide the answer for the long-term stability of PSCs. Also, new possibilities for developing perovskite-based solar cells with high efficiency are achieved.

CHAPTER II

SCAPS-1D

SCAPS-1D

Introduction

SCAPS (Solar Cell Capacitance Simulator) is a numerical software simulator for one-dimensional solar cells, developed by Marc Burgelman from Gent University in Belgium, although it was originally designed to simulate thin-film solar cells of the CuInSe₂ family, CdTe, GaAs and even hybrid perovskite solar cells. This simulator is freely available to the photovoltaic research community, its latest version is SCAPS 3.8 launched in May 2020. An overview of its main features is given as follows:

- We can use only 7 semiconductor layers.
- All the geometrical and physical parameters can be introduced with graded variations: for example, χ , ϵ , N_c , N_v , V_{thn} , V_{thp} , μ_n , μ_p , N_a , N_d ;
- Mechanisms of recombination: band to band (direct), Auger and SRH.
- Defects levels: in volume or at the interface, considering their charge states and recombination at their levels.
- Taps levels, charge type: no charge (neutral), monovalent (only one donor, acceptor), divalent (double donor, double acceptor, amphoteric), multivalent (user defined).
- Defect levels, energy distribution: discrete level, uniform, Gauss, under tail form or a combination.
- Defect levels, optical property: Direct excitation by light is possible (known as photovoltaic impurity effect, IPV).
- Defect levels, metastable transitions between levels.
- Contacts: Metal work function or flat band regime; Optical property (Reflection or transmission) of the filter.
- Tunneling, inter-band (in the conduction band or in the valence band), tunneling to/or from interface states.
- Generation: from an internal calculation or from a $g(x)$ file provided by the user.
- Illumination: on the p or n side.

- Points for work calculations: voltage, frequency, temperature.
- The software calculates the energy bands, concentrations and currents at a point of operation given the characteristics (J-V), the characteristics of the alternating current (C and G as function of V and/or f), the spectral response (also with polarization light or voltage).
- Batch calculations possible, presentation of the results and the parameters according to them.
- Loading and saving of all parameters; starting SCAPS in a custom configuration, a scripting language including a free user function.
- Very intuitive user interface.
- A central scripting language to run SCAPS from an «every script file» Internal variable can be viewed and plotted by the script.
- A built-in curve fitting facility.
- A panel for the interpretation of admission measures

II.1 Software manipulation

SCAPS is a program designed to work under the windows system. When you click on the program icon on the desktop or double-click on the file, the main screen of the SCAPS-1D program appears in figure II.1.

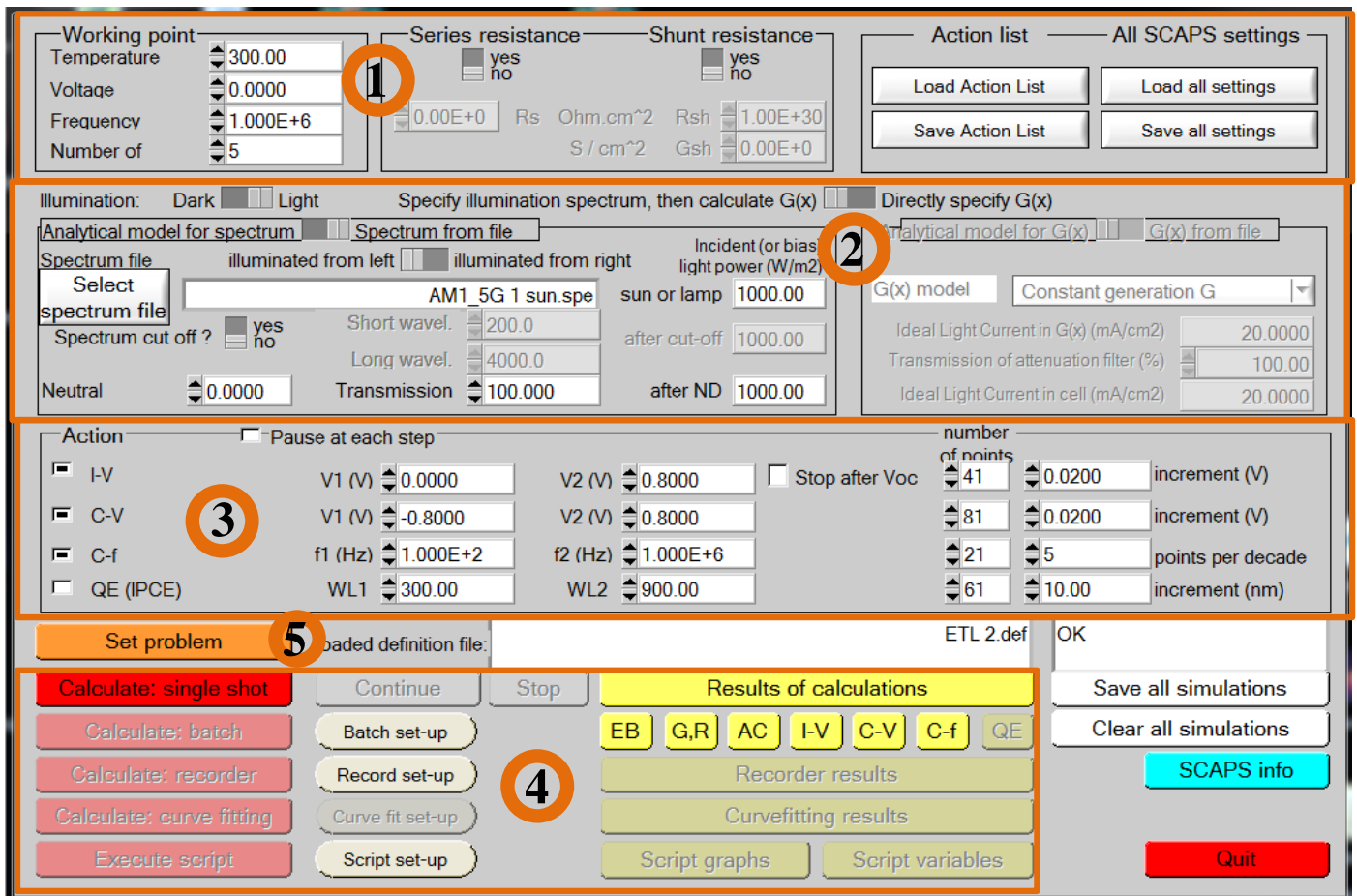


Figure.II.1: Main interface of SCAPS-1D.[30]

II-2 Basic notion:

1. Simulation execution conditions.
2. lighting conditions.
3. Type and parameters of calculation.
4. Calculation and results.
5. Define the problem, as well as the geometry, materials and all properties of the cell solar studied.

II.2.1 Simulation execution conditions:

In this section, the working points are very important and considered as pre-conditions before start simulating the suggested configuration, in which they are defined the desired temperature, frequency, voltage, presence of series resistors and in shunt resistors.

It also consists an important part of what is known working point of four parts as shown in figure II.2

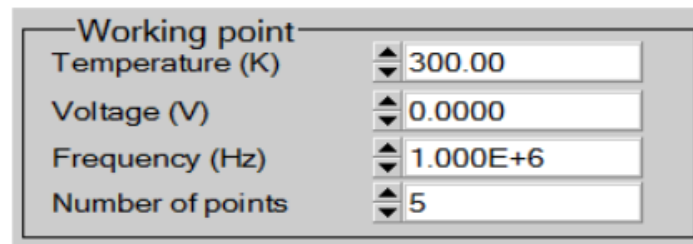


Figure II.2: Working point

* Voltage(V): It is not concerned with simulations J-V and C-V. It is the voltage of the DC polarization in a simulation C-F and QE (λ). SCAPS always starts at 0 V, and runs the voltage of the operating point by a number of steps that must also be specified.

* Frequency (F): It does not relate to J-V, QE (λ) and C-F simulations. This is the frequency in which the characteristic C-V is simulated.

* Illumination: it is used in all measurements. For QE (λ), it determines the conditions of light polarization. The basic parameters are: the darkness or the light, the choice of the illuminated side, the choice of the spectrum. The illumination spectrum on Sun (= 1000 W / m²) with the overall air mass is the default spectrum, but there is also a wide range of monochromatic lights and spectra for more custom simulations. If there is an optical simulator, you can immediately load a generation profile instead of using a spectrum.

II.2.2 Lighting condition:

In this section you define the conditions of illumination that can be in the dark, or rather, allow you to choose from the spectrum of illumination that you want to use as standard 1.5 AMG.

II.2.3 Calculation's type and parameters:

In the action part panel, you can choose one or more measurements to simulate: J-V, C-V, C-f and QE(λ). We can also adjust the initial and final values of the argument, as well as the number of steps.

II.2.4 Calculation and results:

In this section if you give the order to the program to calculate from system defined previously, after the calculations, SCAPS moves to the energy band panel, as shown in

figureII.3. In this panel, we can see the band diagrams, the densities of the free carriers, the current density; at the last point of bias. If you want to display the results for intermediate voltages, we use the stop button in the action panel. We can do display the results by the commands Print, Save Graphs, Show, and the values are then displayed on the screen. You can save the values in a data file. You can switch to one of your custom panels.

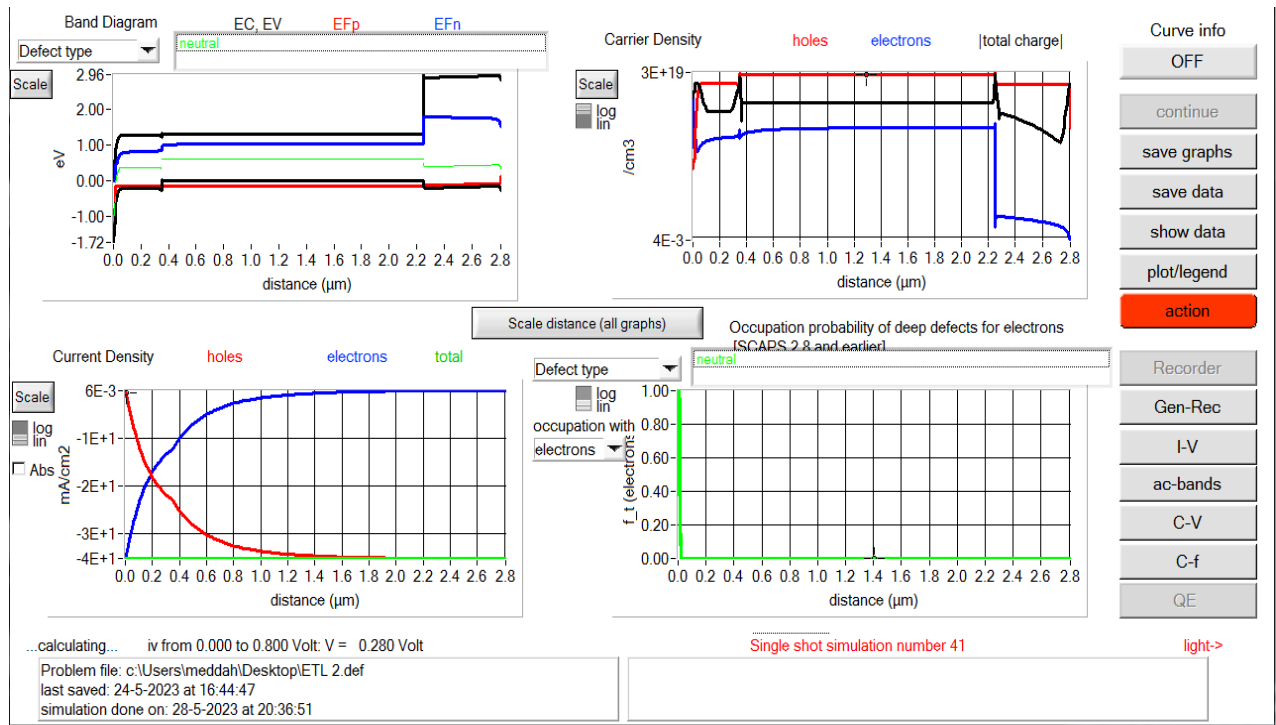


Figure II.3: Energy band panel

II.2.5 Define the problem

By clicking on the set problem bouton and selecting load in the right corner as illustrated in figure II.4, select and open for example: NUMOS CIGS Baseline is an example file of a CIGS-based solar cell. By Subsequently, it is possible to modify all the properties of the cell by clicking on ‘SET PROBLEM’ in the action panel.

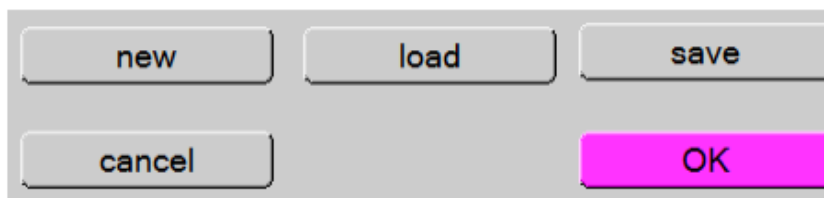


Figure II.4: Define the problem.

II.3 The J-V curves:

The simulation results of the illuminated J-V characteristics are shown in the panel below:

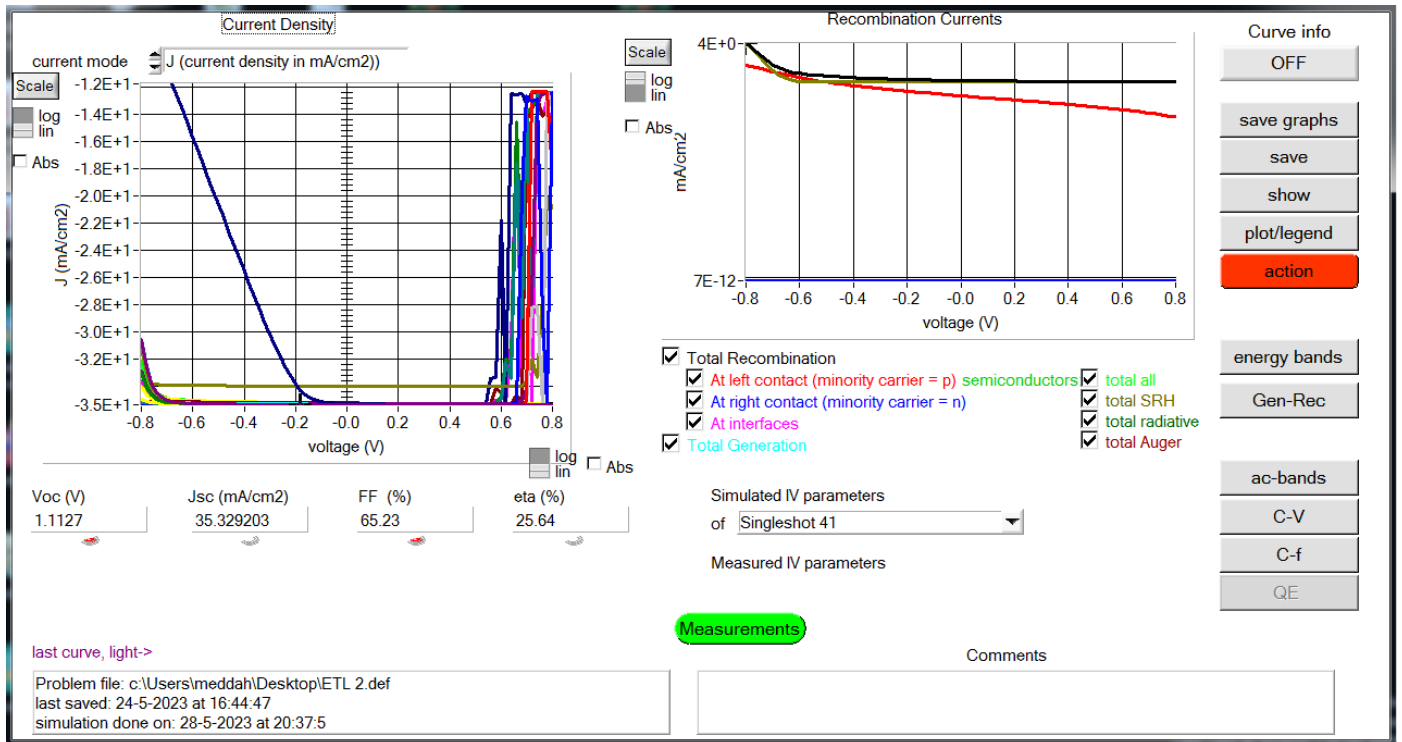


Figure II.5: Panel of simulation results of the Illuminated J-V curve.

The graph on the left shows all J-V simulations. The graph on the right provides detailed information about the recombination currents in the latest simulation, that allows to see the main recombination mechanism in the structure for voltages variables. If the simulation is performed under illumination, the solar cell parameters are calculated and displayed.[30]

II.4 Solar cell editing configuration:

when the ‘Set Problem’ button is clicked on the action panel, the panel ‘Solar Cell Definition’ will be displayed. This will allow you to create or modify the structures of solar cells and save them, or upload them from another files. These definition files are standard ASCII files (American Standard Code for Information Inter change) extension .def which can be opened with Notepad.exe or Wordbad.exe. It is not recommended to modify them at the risk of making them unusable by the following. The layer, contact and interface properties can be modified by clicking on the appropriate button as shown in figure II.6. Similarly, layers can be added by clicking ‘Add Layer’.

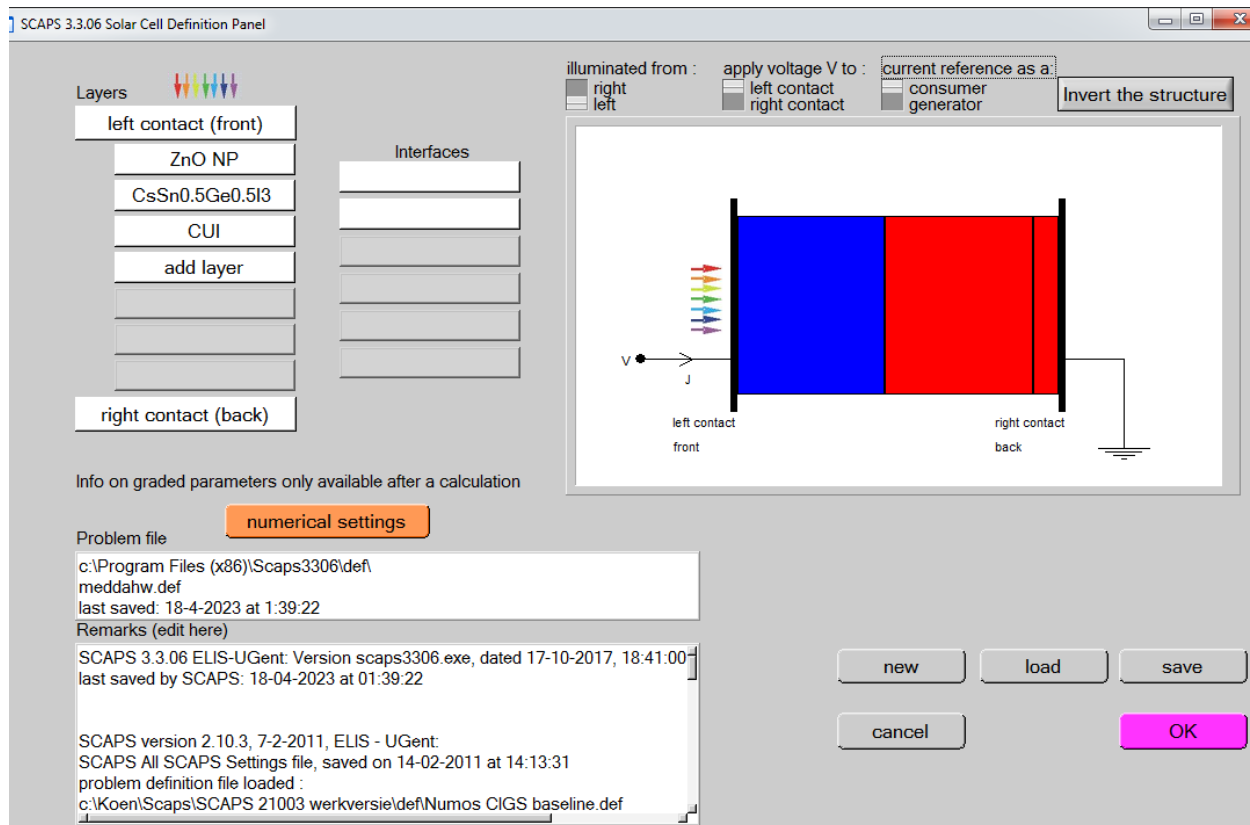


Figure II.6: Definition of layers in SCAPS

II.4.1 Definition of layers:

The total number of layers in the Scaps-1D program is seven layers. We can use all or some of them (3 layers or more). By clicking on the “Add Layer” button, a new window opens, figure II.7 containing a file that includes different information from the materials to be entered, and this information can have uniform or non-uniform distributions according to the physics of the material.

LAYER 1 WS2

thickness (µm) 0.015

uniform pure A (y=0)

The layer is pure A: y = 0, uniform 0.000

Semiconductor Property P of the pure material pure A (y = 0)

bandgap (eV) 1.800

electron affinity (eV) 3.950

dielectric permittivity (relative) 13.900

CB effective density of states (1/cm³) 2.000E+18

VB effective density of states (1/cm³) 2.000E+15

electron thermal velocity (cm/s) 2.000E+5

hole thermal velocity (cm/s) 1.000E+7

electron mobility (cm²/Vs) 1.000E+2

hole mobility (cm²/Vs) 1.000E+2

Allow Tunneling

effective mass of electron 1.000E+0

effective mass of holes 1.000E+0

no ND grading (uniform)

shallow uniform donor density ND (1/cm³) 1.000E+17

no NA grading (uniform)

shallow uniform acceptor density NA (1/cm³) 1.000E+9

Absorption model

alpha (y=0) from model

absorption constant A (1/cm eV^{1/2}) 9.129E+4

absorption constant B (eV^{1/2}/cm) 0.000E+0

show save absorption file for y = 0

Recombination model

Band to band recombination

Radiative recombination coefficient (cm³/s) 0.000E+0

Auger electron capture coefficient (cm⁶/s) 0.000E+0

Auger hole capture coefficient (cm⁶/s) 0.000E+0

Recombination at defects: Summary

Defect 1

Defect 1

charge type : neutral

total density (1/cm³): Uniform 1.000e+15

grading Nt(y): uniform

energydistribution: single; Et = 0.60 eV above EV

this defect only, if active: tau_n = 5.0e+03 ns, tau_p = 1.0e+02 ns

this defect only, if active: Ln = 3.6e+01 µm, Lp = 5.1e+00 µm

Edit Defect 1 Add a Defect 2

Remove

(no metastable configuration possible)

Accept cancel Load Material Save Material

Figure II.7: Added layer properties

In the first box, we introduce the name of the layer (which corresponds to the type of doping). In the second box, the thickness of the layer is entered and the third block concerns the purity of the material and its profile.

In the fourth block, we introduce: the energy gap, the electronic affinity, the permittivity electric, the effective densities of the conduction and valence bands, thermal velocities of the free electrons and holes, the mobilities of electrons and holes, last box makes it possible to add the effective masses of the electrons and the holes if one takes into account the transport of carriers by tunnel effect.

In the fifth block presented in figure II.8 which introduce the doping, type and density. Doping can also be introduced as being uniform, as it may have graded variations (linear, parabolic, etc.).

no ND grading (uniform)	
shallow uniform donor density ND (1/cm ³)	1.000E+15
no NA grading (uniform)	
shallow uniform acceptor density NA (1/cm ³)	1.000E+15

Figure II.8: Properties of defined doping

In the sixth block, we define the absorption of the layer, as shown in figure II.9. Absorption can be defined by the analytical model provided by SCAPS, as it can be introduced as data. SCAPS provides a number of absorption data for several types of semiconductors. Other absorption data can also be used for semiconductors is not available in SCAPS, provided the file has the same extension of the absorption files provided by SCAPS.

Absorption model	
	alpha (y=0) <input type="checkbox"/> from model <input checked="" type="checkbox"/> from file
absorption constant A (1/cm eV ^{1/2})	1.000E+5
absorption constant B (eV ^{1/2} /cm)	0.000E+0
<input type="button" value="show"/> <input type="button" value="save"/> <input type="button" value="absorption file for y = 0"/>	

Figure II.9: Absorption model

The type of volume recombination present is indicated in the right side of the panel of layer properties as illustrated in figure II.10. All types of recombination are present; direct or through the traps.

Recombination model	
Band to band recombination	
Radiative recombination coefficient (cm ³ /s)	0.000E+0
Auger electron capture coefficient (cm ⁶ /s)	0.000E+0
Auger hole capture coefficient (cm ⁶ /s)	0.000E+0
Recombination at defects: Summary	

Figure II.10: Recombination mode

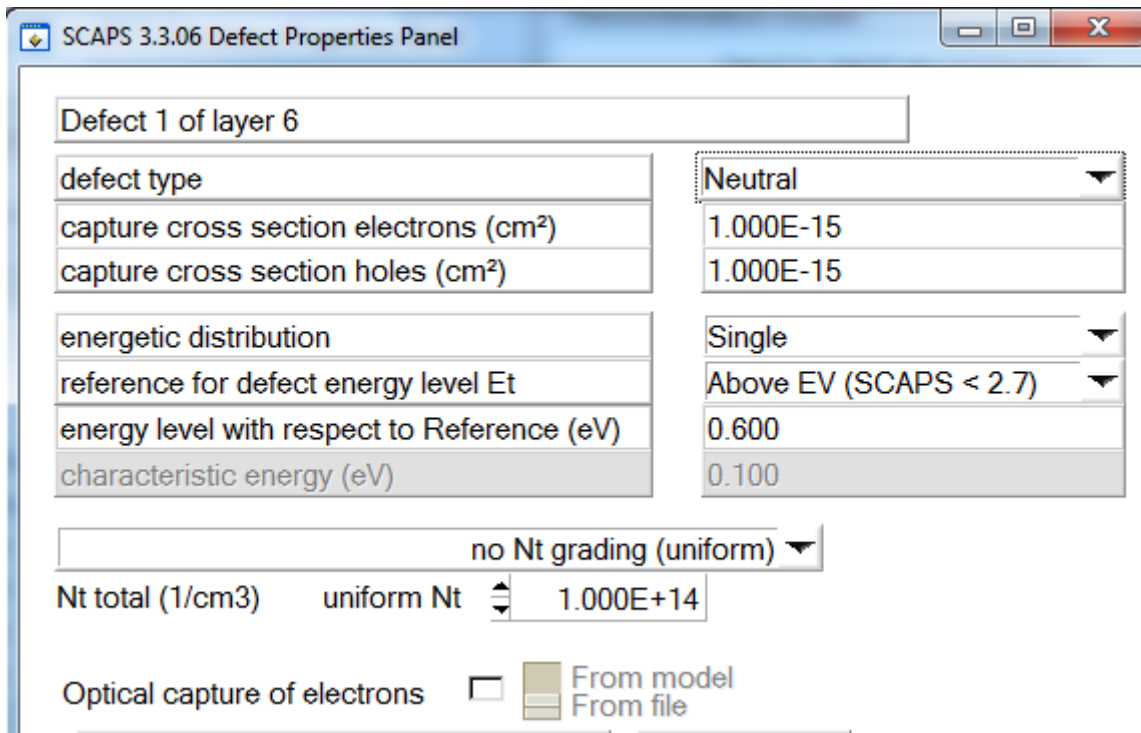


Figure II.11 Recombination types definition.

If we introduce defects (traps); AS shown in figure II.11 they can be uniform or non-uniform, discrete, with gaussian distributions, donors, acceptors, neutral, monovalent or divalent. We can even define carrier transitions between the different energy levels of the traps.

II.4.2 Contacts:

By clicking the front contact or back contact button on the cell identification panel the connection properties can be entered.

A panel of contact properties ‘Contact Properties Panel’ opens, as shown in figure II.11

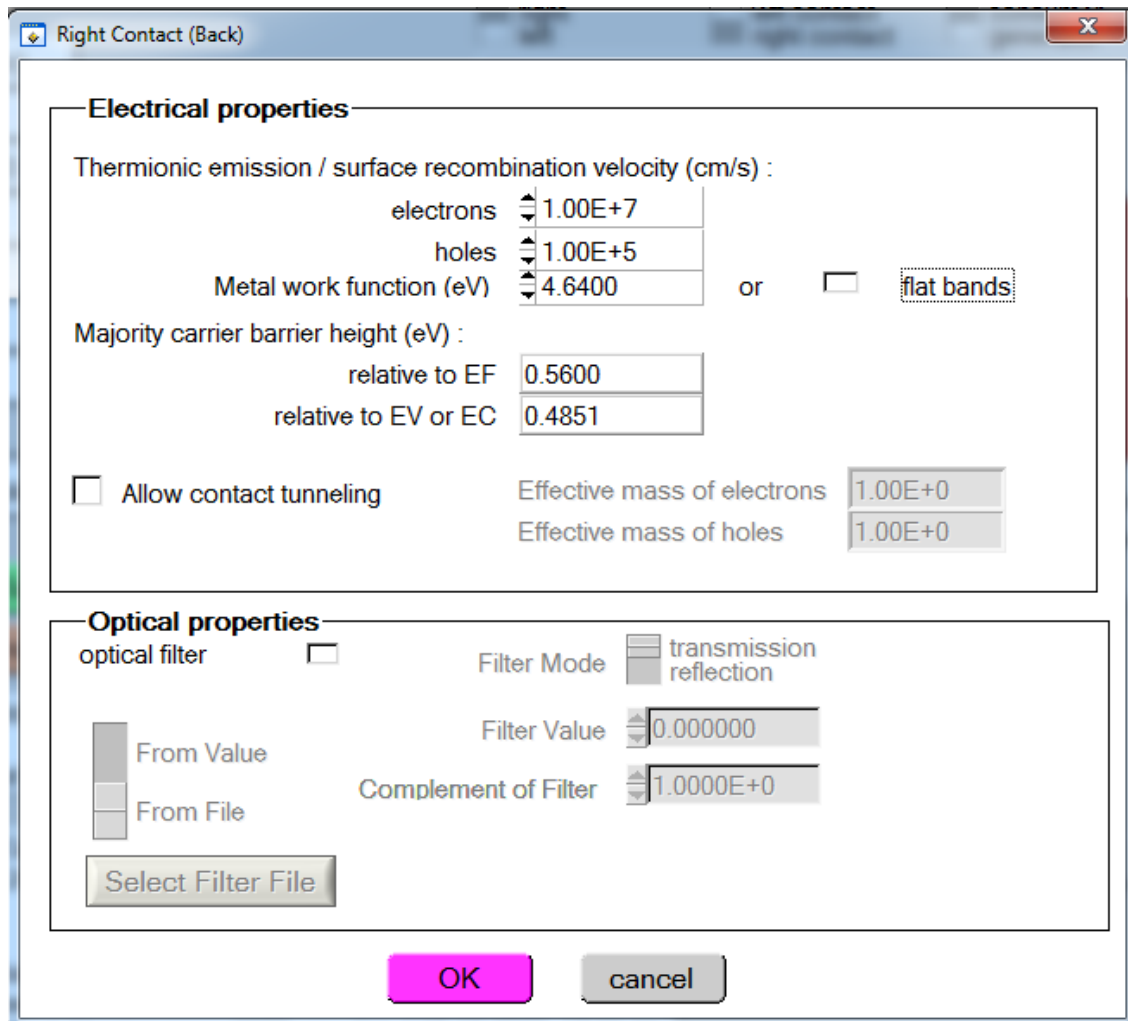


Figure II.12: Contact properties panel.

The properties of contacts are electrical and optical:

for the electrical properties, we define:

- Surface recombination velocities of free electrons and holes.
- If the contact has a work function, or it is ideal (flat band regime).
- The majority carrier barrier.
- The tunnel effect (if we want to take it into account).
- For optical properties, transmission or reflection can be defined by a value or a data file.

For optical properties, transmission or reflection can be defined by a value or a data file.

Conclusion:

In this chapter, we've covered everything related to SCAPS software, including features and tools.

CHAPTER III

RESULTS AND DISCUSSION

RESULTS AND DISCUSSION

CHAPTER III

Introduction:

Major drawback that has so far hindered the exploitation of solar energy photovoltaic is the cost of solar panels. Therefore, the main objective of researchers is to improve the power conversion efficiency of solar cells as well as reduce their manufacturing costs. For perovskite cells, it will be interesting to reduce the amount of absorber material, which requires a material with a large absorption coefficient and excellent carrier mobility. In this chapter, we are interested in the study and simulation of solar cells-based perovskite materials, The aim is to maximize the power conversion efficiency of the proposed configuration of solar cell, the following numerical simulation based on the optimization of the input parameters to increase as maximum as possible the PCE.

III.1 Structure of the studied cell:

Our work is study and optimization of the graded approach for boosting up the power conversion efficiency in solar cell-based perovskite via numerical simulation of the suggested structure of IGZO/CsSn0.5Ge0.5I3/CsSnCl3/CsSnCl3/CuO2/Spiro-OMeTAD, in the way of simulating the electrical, optical and geometric parameters in order to obtain the best values of V_{oc} , J_{sc} , FF and PCE. The used configuration is a planar n-i-p, where the absorbent layer (CsSn0.5Ge0.5I3, CsSnCl3, CsSnCl3) are inserted as sandwiches form between a layer n -type ETL consisting of (IGZO) and HTL layers of p -type consisting of (CuO2). In a perovskite solar cell, the HTL layer plays an important role in improving performance, it allows easier transport of layer holes to back contact. A schematic view of perovskite simulated in this work is presented in Figure III.1.

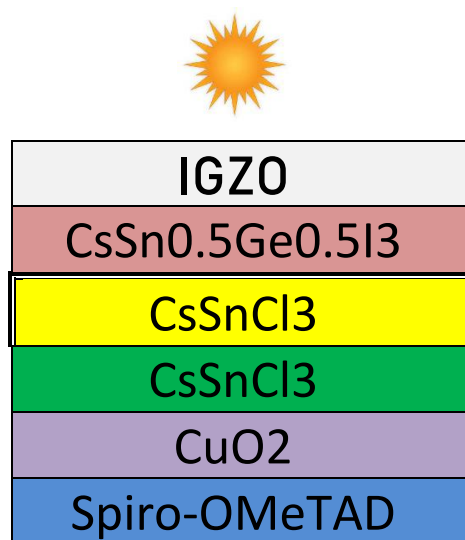


Figure III.1: Structure of the suggested solar cell-based perovskite.

III.1.1 Parameters of the studied perovskite cell:

The following table III.1 presents all used parameters in proposed structure of IGZO/CsSn0.5Ge0.5I3/CsSnCl3/CsSnCl3/CuO2/Spiro-OMeTAD.

Parameters	IGZO [31]	CsSn0.5 Ge0.5I3 [32]	CsSnCl3 [31]	CsSnCl3 [31]	Cu2O [31]	Spiro- OMeTAD [33]
Thickness (um)	0.015	0.250	1.000	1.000	0.400	0.100
Band gap (eV)	3.050	1.498	1.240	1.220	3.700	4.005
Electron affinity (eV)	4.160	4.000	3.800	3.700	1.700	1.460
Dielectric Permittivity	10.00	28.000	20.000	20.000	10.000	10.700
CB effective density of states (1/cm ³)	5.000E+21	3.100E+18	5.000E+16	5.000E+16	2.200E+19	2.800E+20
VB effective density of states (1/cm ³)	5.000E+16	3.100E+19	5.000E+16	5.000E+16	1.800E+18	1.000E+20
Electron mobility (cm ² /VS)	1.500E+1	9.740E+2	5.000E+1	7.000E+1	1.000E+2	1.200E+1
Hole mobility (cm ² /VS)	1.000E-1	2.130E+2	5.000E+1	5.000E+1	2.500E+1	2.800E+0
Shallow uniform donor density N _D (1/cm ³)	1.000E+18	0.000E+0	0	0	0	0
Shallow uniform acceptor density N _A (1/cm ³)	1.000E+5	1.100E+18	1.000E+20	1.000E+210	2.000E+21	1.000E+21

Table III.1: Properties of the different layers of the proposed structure

Table III.2 and III.3 present the used ETL and HTL in suggested model

ETL Parameters	WS2 [34]	CdS [31]
Thickness (um)	0.015	0.020
Band gap (eV)	1.800	2.420
Electron affinity (eV)	3.950	4.300
Dielectric Permittivity	13.900	9.350
CB effective density of states (1/cm ³)	2.000E+1 8	2.200E+ 17
VB effective density of states (1/cm ³)	2.000E+1 5	1.800E+ 17
Electron mobility (cm ² /VS)	1.000E+2	1.00E+2
Hole mobility (cm ² /VS)	1.000E+2	2.500E+ 1
Shallow uniform donor density N _D (1/cm ³)	1.000E+1 7	1.000E+ 18
Shallow uniform acceptor density N _A (1/cm ³)	1.000E+9	0

Table III.2: Used ETL Parametres

HTL Parameters	P3HT [34]	CuI [32]
Thickness (um)	0.400	0.400
Band gap (eV)	1.700	3.100
Electron affinity (eV)	3.500	2.100
Dielectric Permittivity	5.000	6.500
CB effective density of states (1/cm ³)	2.000E+2 0	2.200E +19
VB effective density of states (1/cm ³)	2.000E+2 0	1.800E +19
Electron mobility (cm ² /VS)	1.800E-2	4.390E +1
Hole mobility (cm ² /VS)	1.860E-2	2.000E- 4
Shallow uniform donor density N _D (1/cm ³)	0	0.000E +0
Shallow uniform acceptor density N _A (1/cm ³)	5.000E+1 7	1.000E +18

Table III.3:Used HTL Parametres

III.2 ETLs effect on the solar cell performance:

In a perovskite solar cell, the ETL layer plays an important role in improving performance, it facilitates the transport of electrons from perovskite layer to the front contact. In this part we will study the influence of the ETL thickness on output performance.

III.2.1 Thickness effect:

As presented in figure III.2, the output parameters functions of thickness of ETL to see its impact on J_{sc} , V_{oc} , FF and PCE. According to the efficiency, we notice that thickness of $0.02 \mu m$ related to the best value of PCE (28.3%) which is obtained from the multiplication of $J_{sc} \times V_{oc} \times FF$ ($38.4 \text{ mA/cm}^2 \times 1.225 \text{ V} \times 60.25\%$), the IGZO material shows a good efficiency comparing to WS2 and Cds.

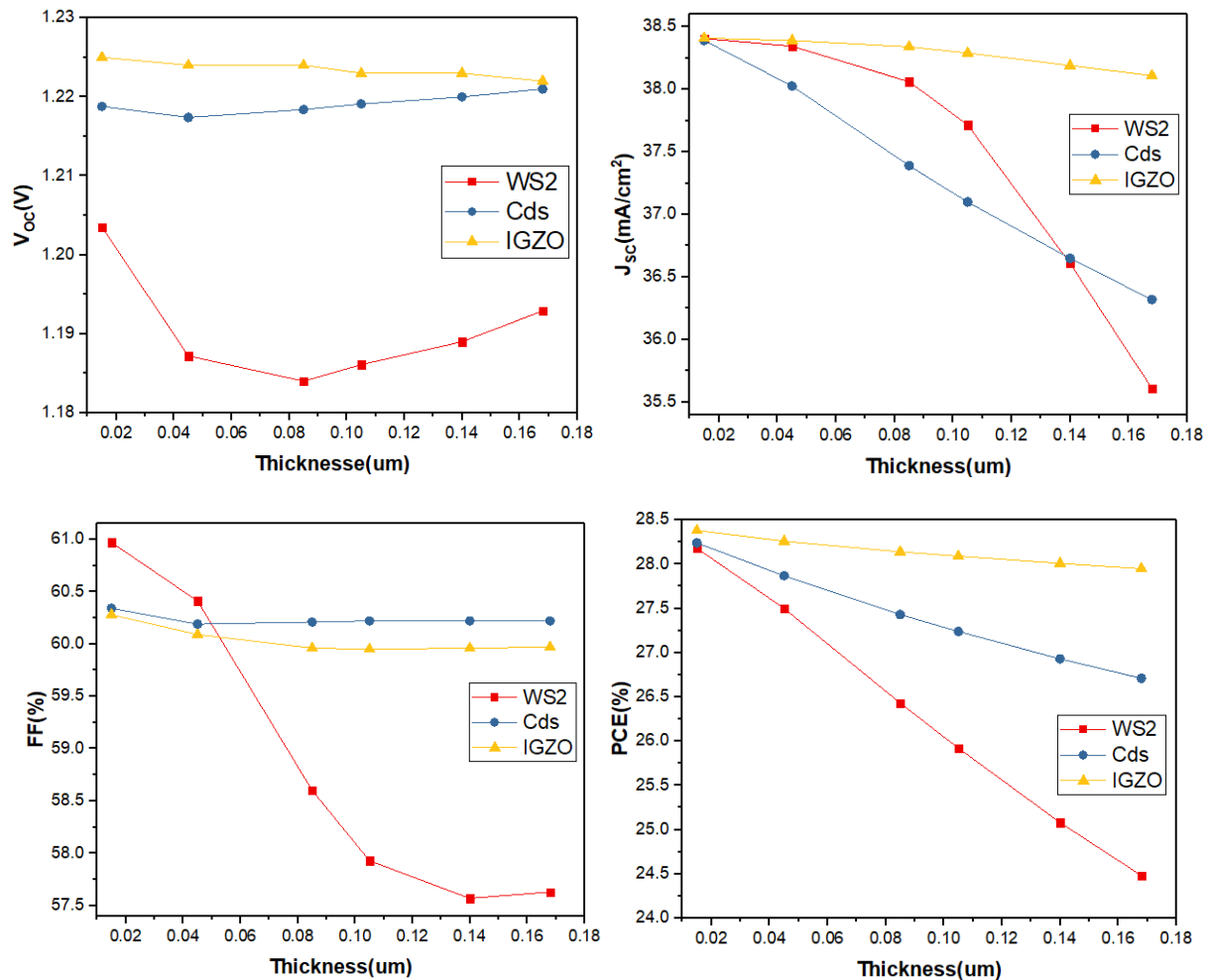


Figure III.2: Thickness effect of ETL layer on performance solar cell

III.2.2 Doping effect:

In figure III.3, the output parameters versus the variation of defect density from 6×10^{16} to 1×10^{18} . The output parameters show a constant variation except J_{sc} gives its better values at the doping of 1×10^{17} for 38.415 Ma/cm^2 .

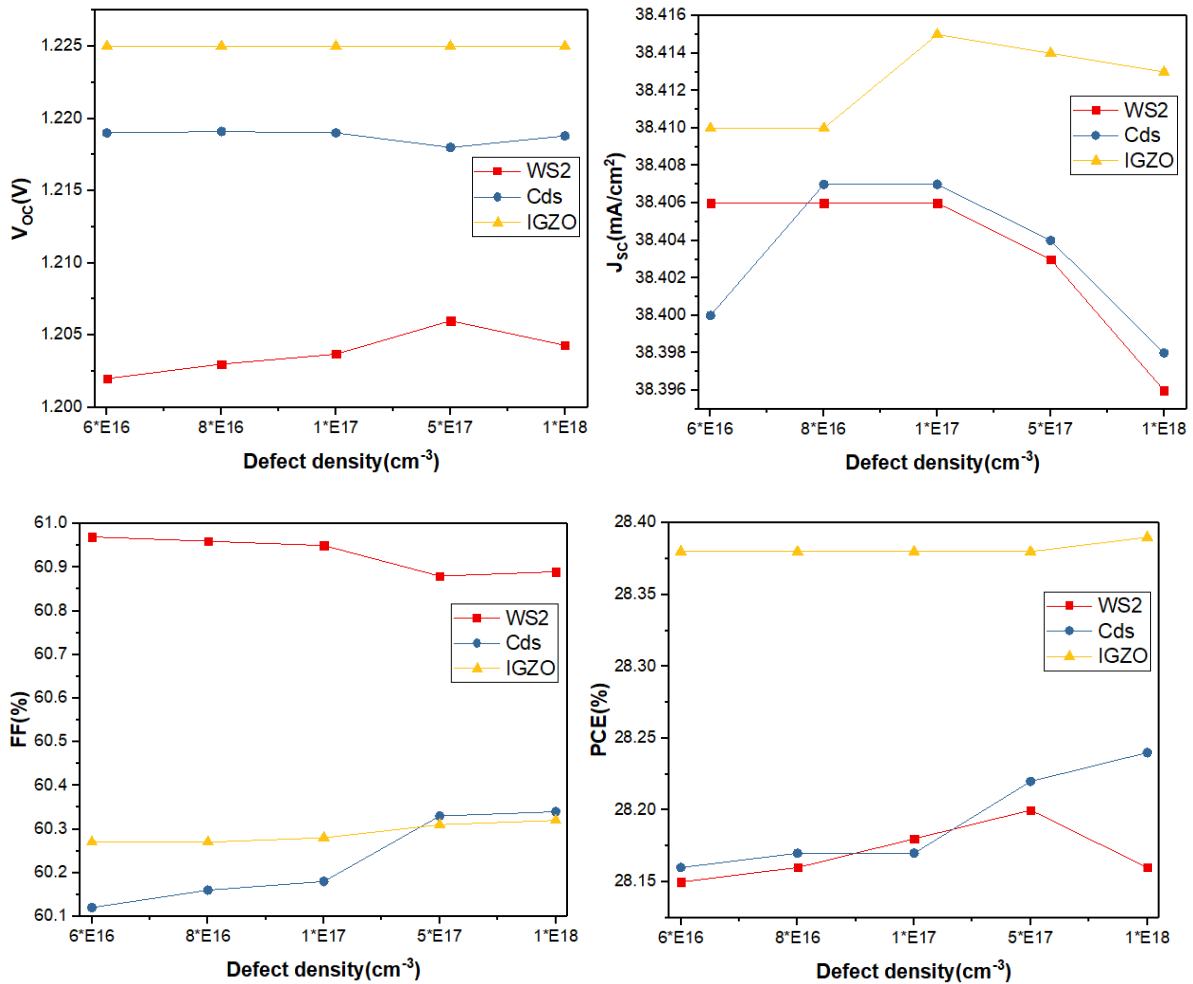


Figure III.3: Doping effect of ETL layer on performance solar cell

III.3 Perovskite effect on the solar cell performance:

The effect of thickness and doping of the absorber layer are necessary to study the output parameters of the desired structure.

III.3.1 Thickness effect of the first perovskite layer (CsSn0.5Ge0.5I3):

Figure III.4 depicted the variation of the output photovoltaic parameters (V_{oc} , J_{sc} , FF and PCE) as function of the thickness of the first perovskite layer (CsSn0.5Ge0.5I3). The present simulation gives the best PCE of 28.575 % in the thickness of $0.25 \mu\text{m}$ and up to that will decrease just like V_{oc} , but J_{sc} and FF increase up to the same value of $0.25 \mu\text{m}$.

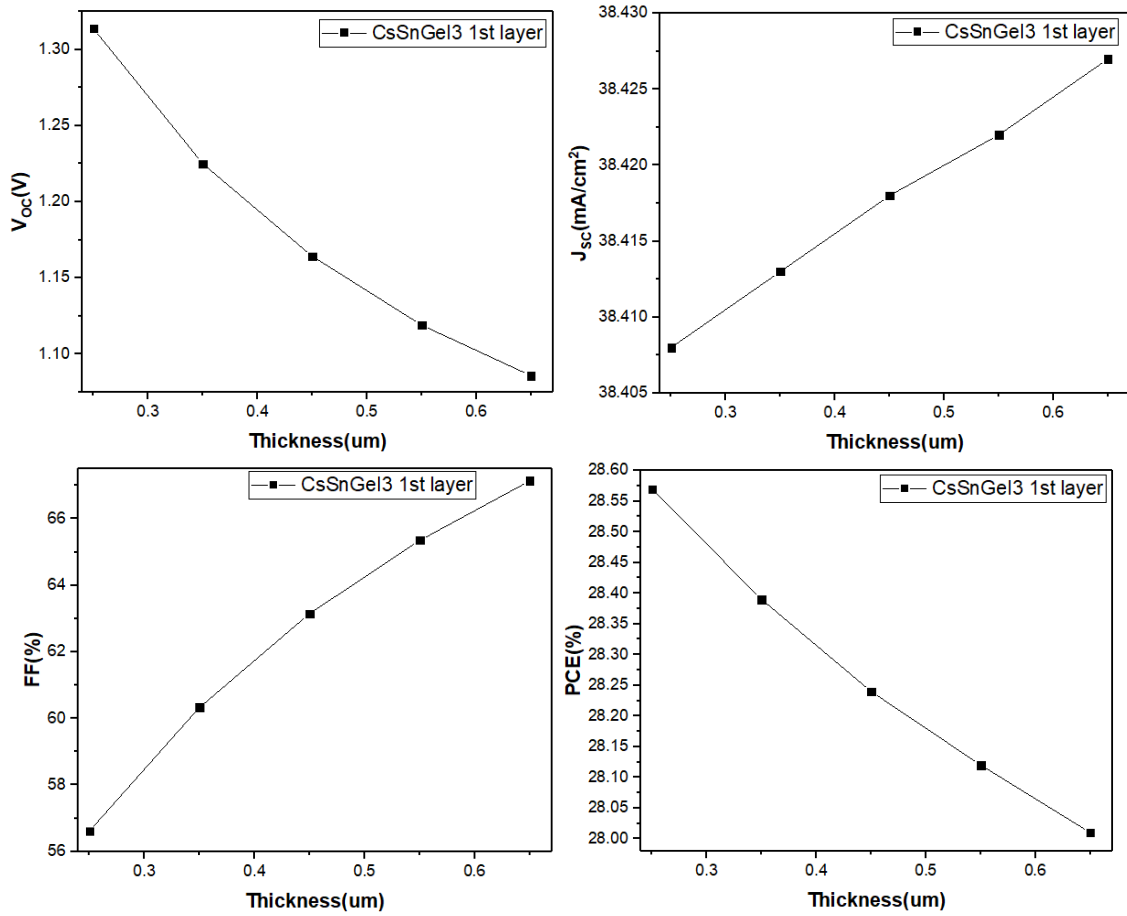
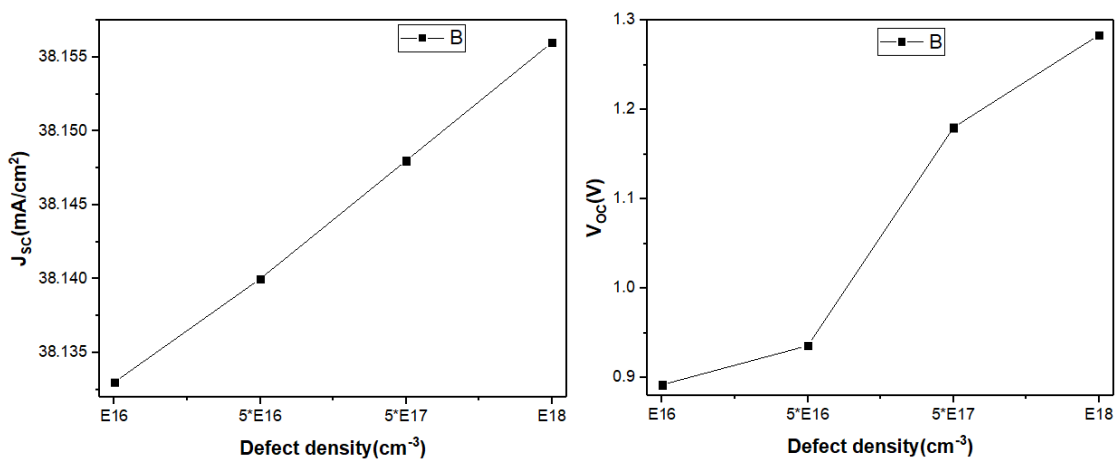


Figure III.4: Thickness effect of first perovskite layer on performance solar cell

III.3.2 Doping effect of first perovskite layer (CsSn0.5Ge0.5I3):

In this part we will see the effect of doping for the first perovskite layer as shown in figure III.5



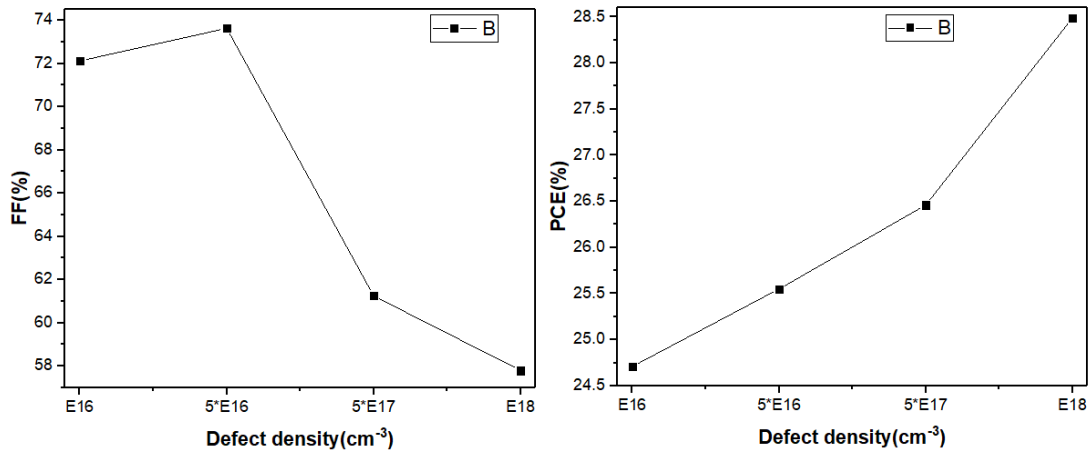


Figure III.5: Doping effect of the first perovskite layer on the output parameters.

We observe that the PCE arise to reach its best value of 28.5% at the defect density of E18 cm⁻³ and the same for J_{SC} and V_{OC}, but FF gets its best value at 5×E16 cm⁻³ then, decreases.

III.3.3 Thickness effect of the second perovskite layer (CsSnCl3):

In Figure III.6, the variation of the output parameters versus thickness of the second perovskite layer. The PCE proportionally increasing with thickness and stabilized up to 0.9 μm for PCE of 28.52 %.

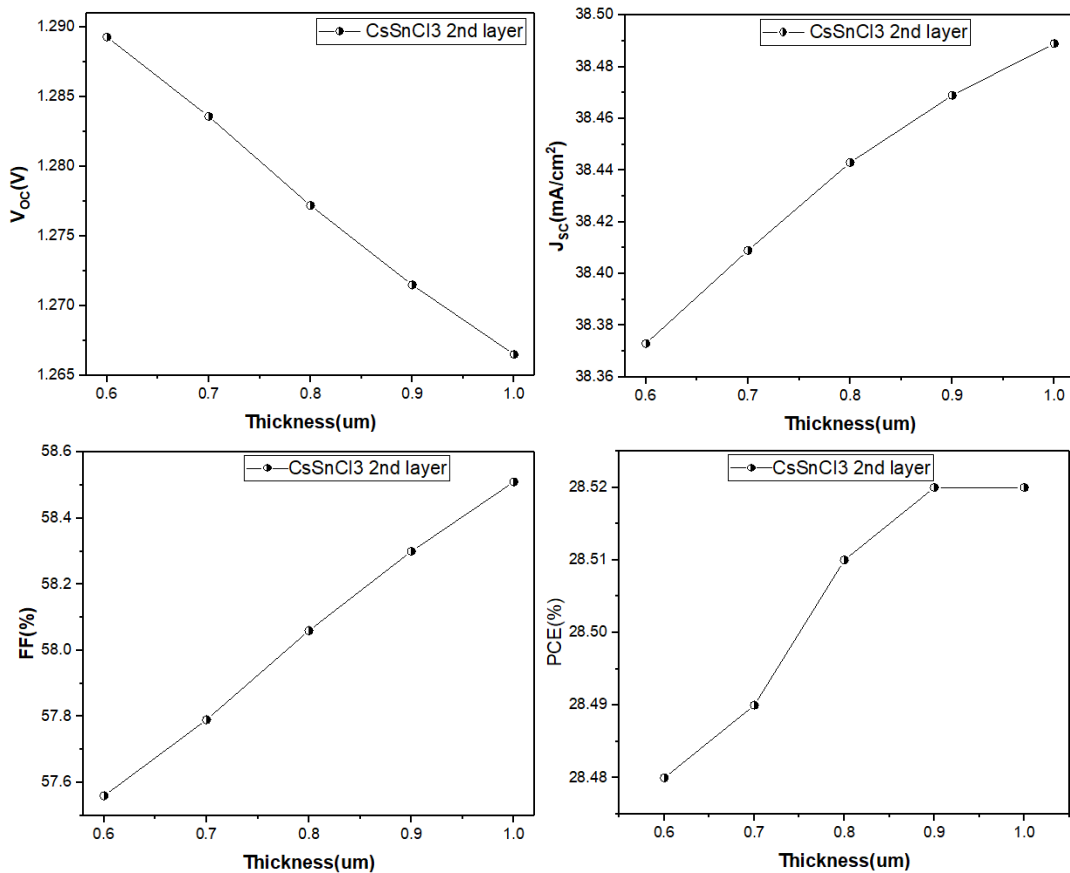


Figure III.6: Thickness effect of second perovskite layer on performance solar cell.

III.3.4 Doping effect of second perovskite layer (CsSnCl₃):

As presented in the following Figure III.7. we study the influence of defect density on the output parameters, the defect density varies from $E18 \text{ cm}^{-3}$ to $E21 \text{ cm}^{-3}$, the PCE best value localized at $E20 \text{ cm}^{-3}$ of 28.6 %.

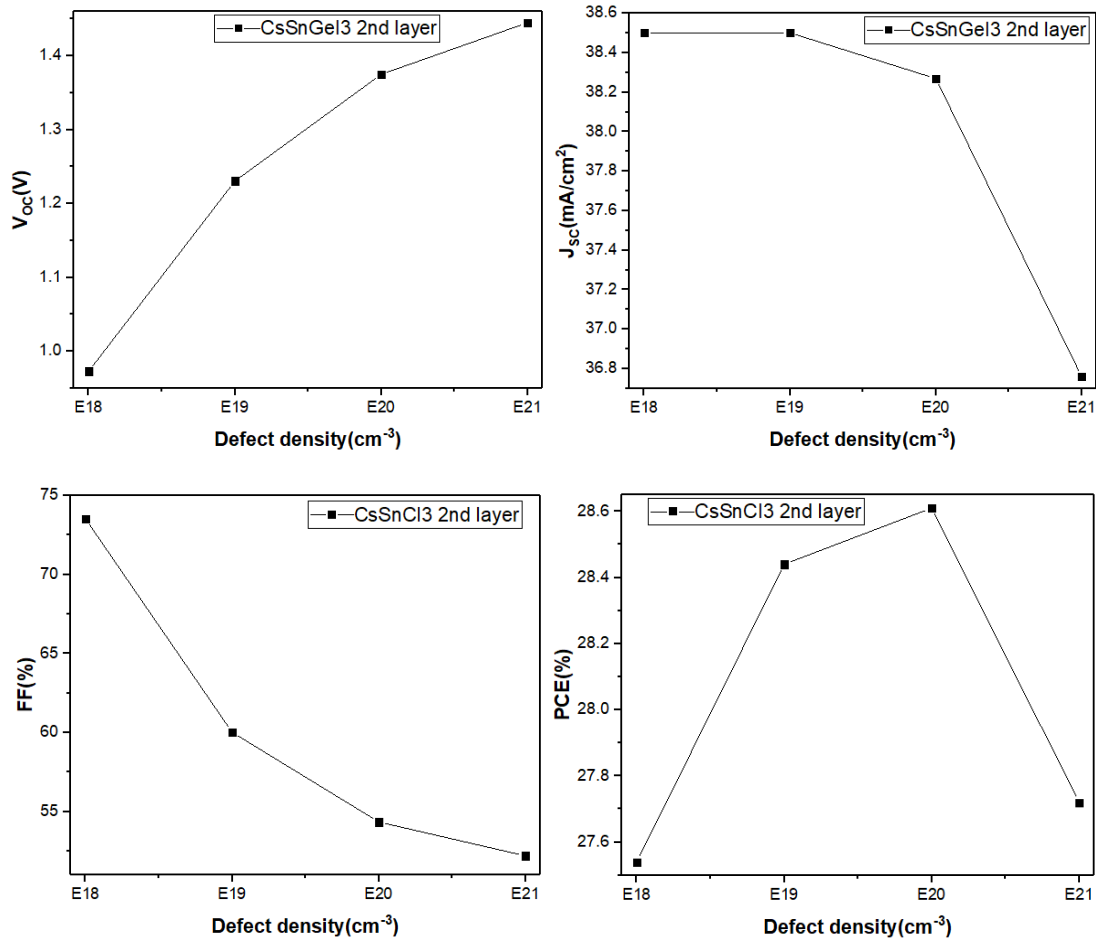


Figure III.7: Doping effect of second perovskite layer on performance solar cell

III.3.5 Thickness effect of the third perovskite layer (CsSnCl₃):

As illustrated in figure III.8, the performance of the solar cell based on the variation of thickness for the third perovskite layer. The device demands the integration by getting its best PCE value of 28.63 % at the thickness of $1 \mu\text{m}$.

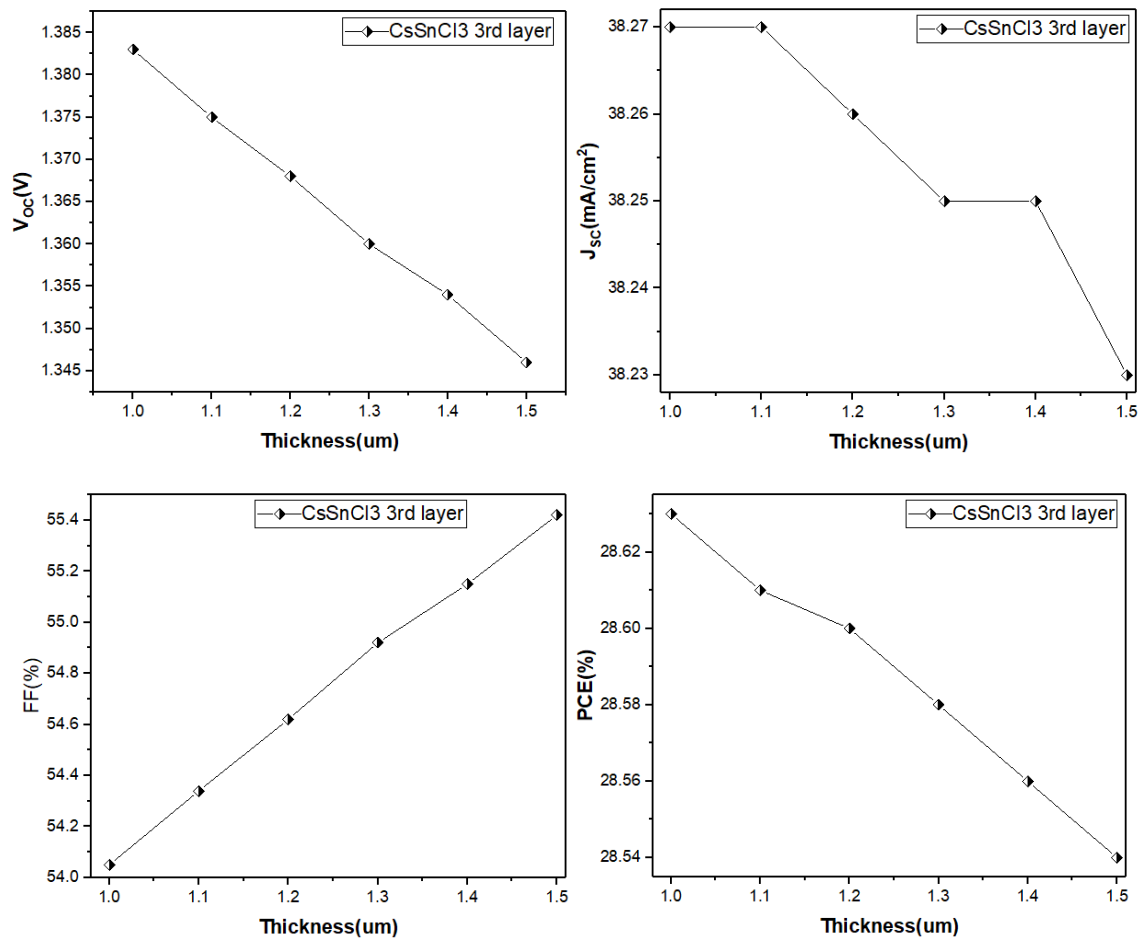


Figure III.8: Thickness effect of third perovskite layer on performance solar cell

III.3.6 Doping effect of the third perovskite layer (CsSnCl3):

In figure III.8, the output parameters show the best value of PCE of 28.9% at a defect density of $E21\text{ cm}^{-3}$, and in the same defect density the short-circuit current shows 28.51 mA/cm², the open-circuit voltage has a 1.48 V and the fill factor has 67.1%.

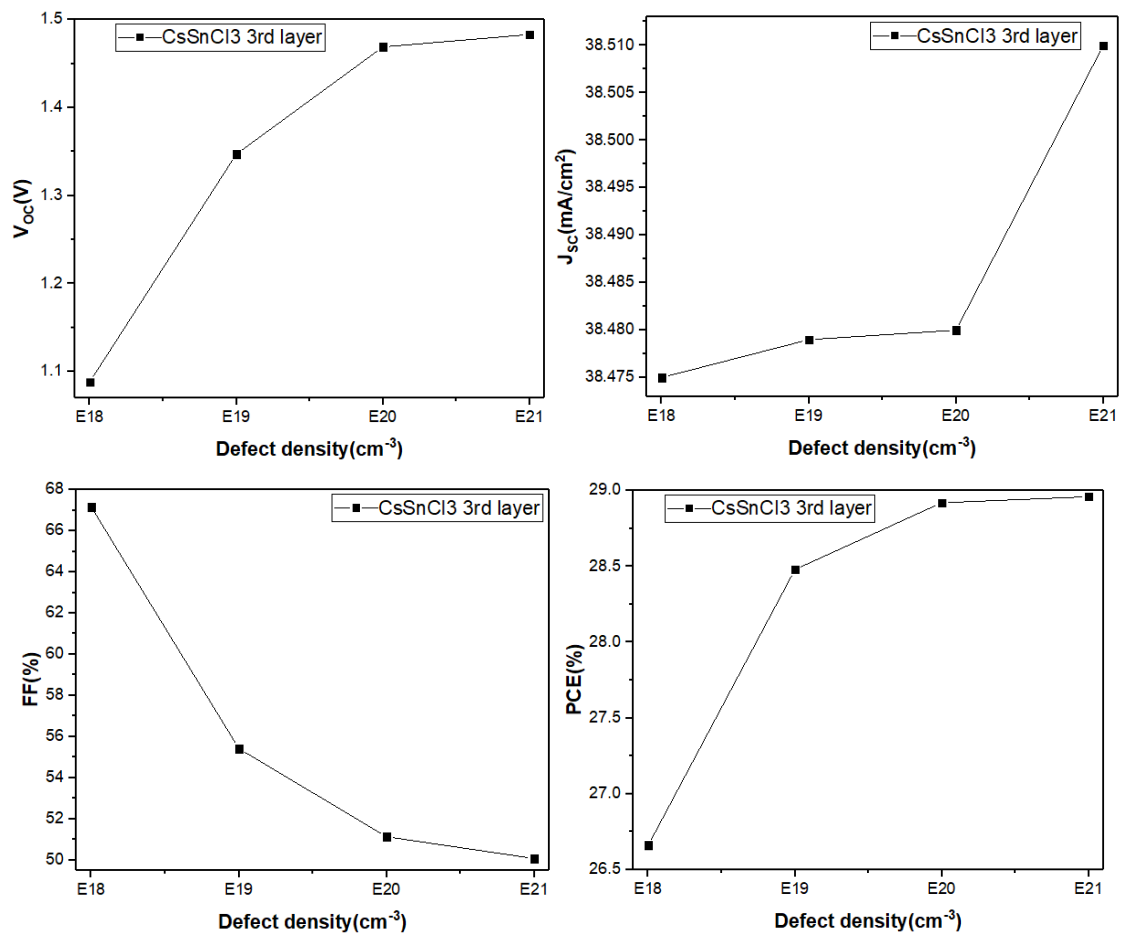


Figure III.9: Doping effect of third perovskite layer on performance solar cell

III.4 HTL effect on the solar cell performance:

In solar cell-based perovskite, the HTL layer plays an important role in improving performance, it allows easier transport of electrons holes to the back contact. In this section we will study the effect of thickness and doping of the HTL layer on the solar cell performance.

III.4.1 Thickness effect

As illustrated in figure III.10, thickness of HTL has an excellent role for improving the performance of the solar cell, different simulation of Cu₂O, CuI and P3ht are done.

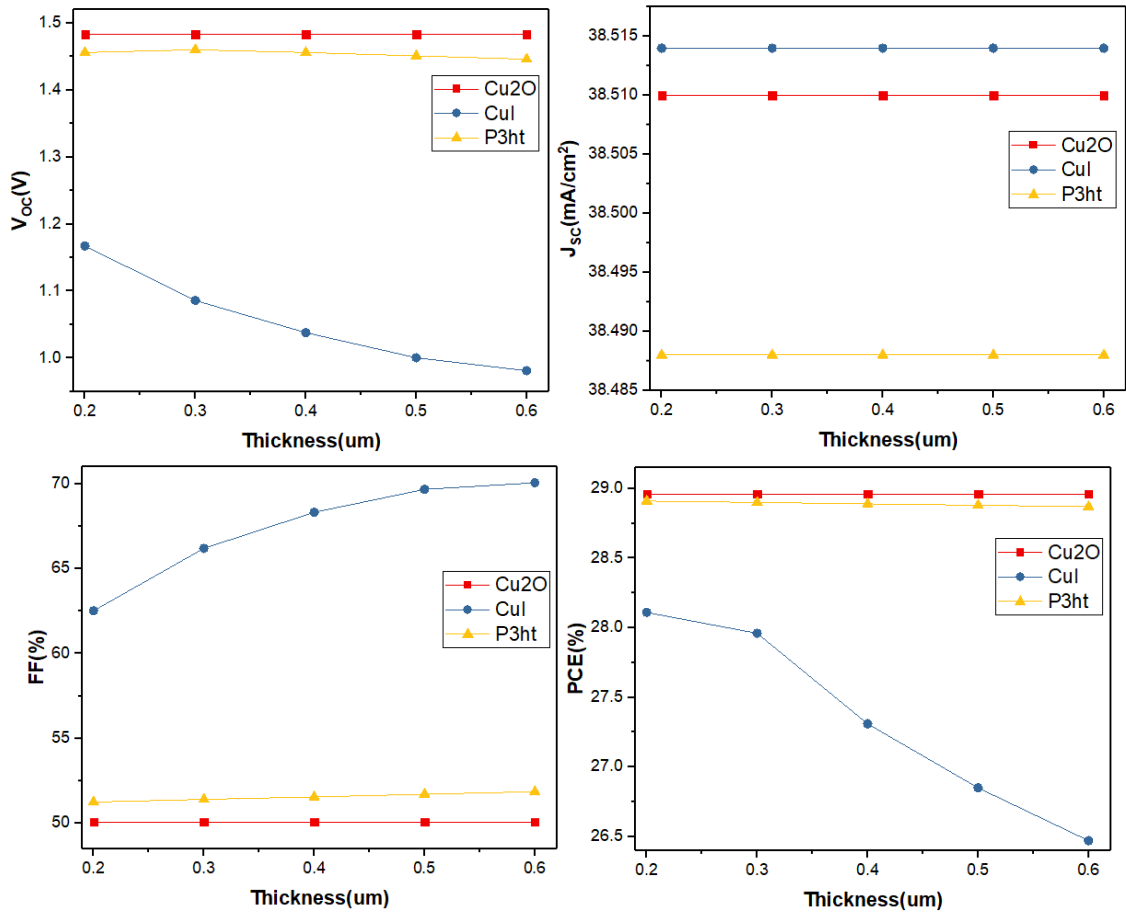
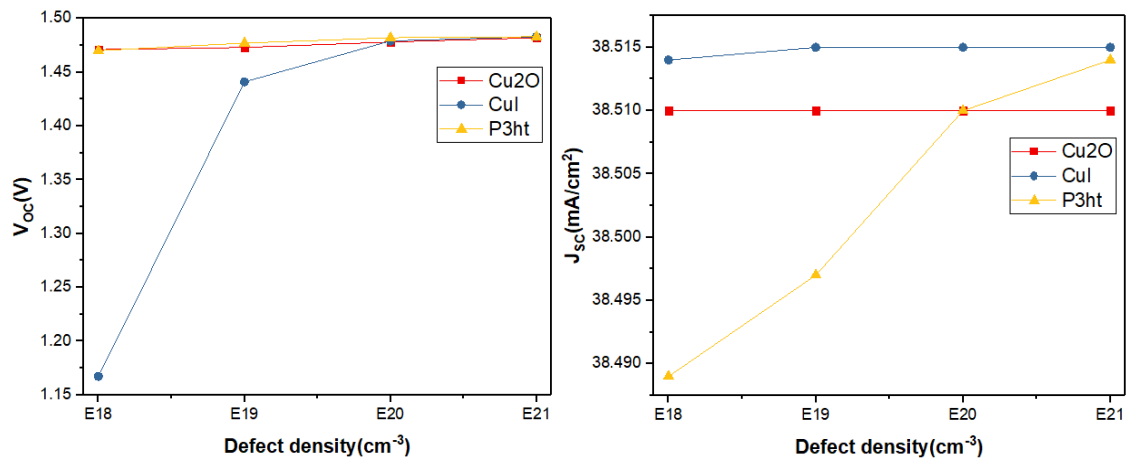


Figure III.10: Thickness effect of HTL layer on performance solar cell

III.4.2 Doping effect:

From the simulation results, it is therefore clear that among the three materials Simulated HTL Cu₂O is the HTL material that offers the best performance photovoltaic. It is by considering Cu₂O as the material of the transport layer of holes that we could obtain the highest efficiency of 28.95 for the thickness and efficiency of 28.90 for the doping.



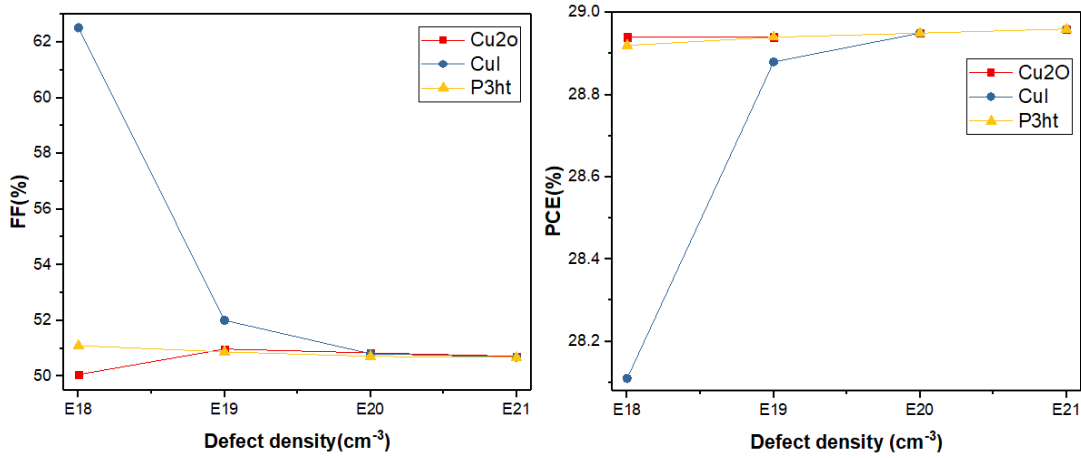


Figure III.11: Doping effect of HTL layer on performance solar cell

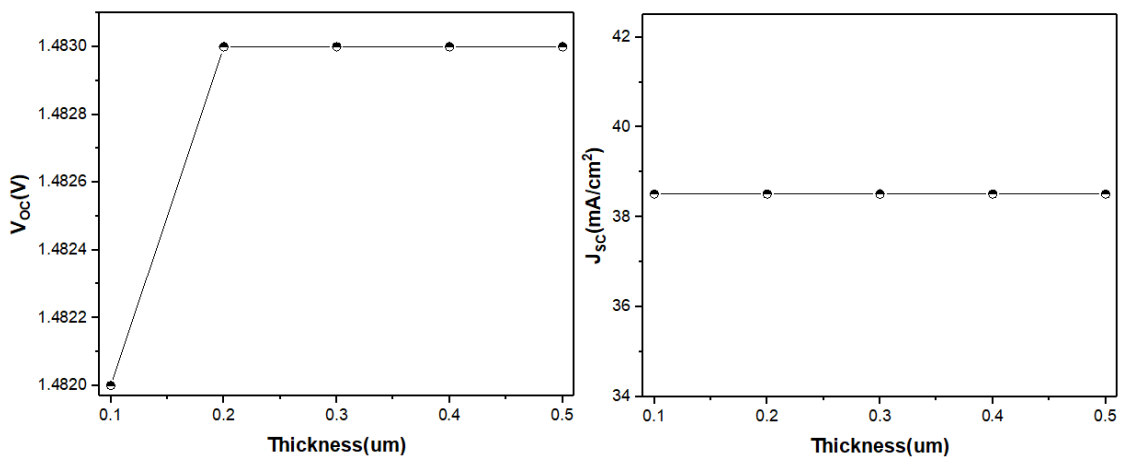
III.5 BSF effect on the solar cell performance:

Between the back contact and the HTL, Back Surface Field (BSF) has been used as one of means to enhance solar cell performance by reducing surface recombination velocity (SRV). One of methods to produce BSF is by introducing highly doped layer on rear surface of the wafer. Depending on the type of the dopant in wafer, the BSF layer could be either p⁺ or n⁺. This research aims to compare the performance of BSF layer for the p-type.

III.5.1 Thickness effect

As presented in figure III.2, the variation of output parameters versus thickness of BSF.

The effect of thickness in the BSF layer shows a constant value up to 0.2um for all output parameters, the efficiency PCE≈29 %.



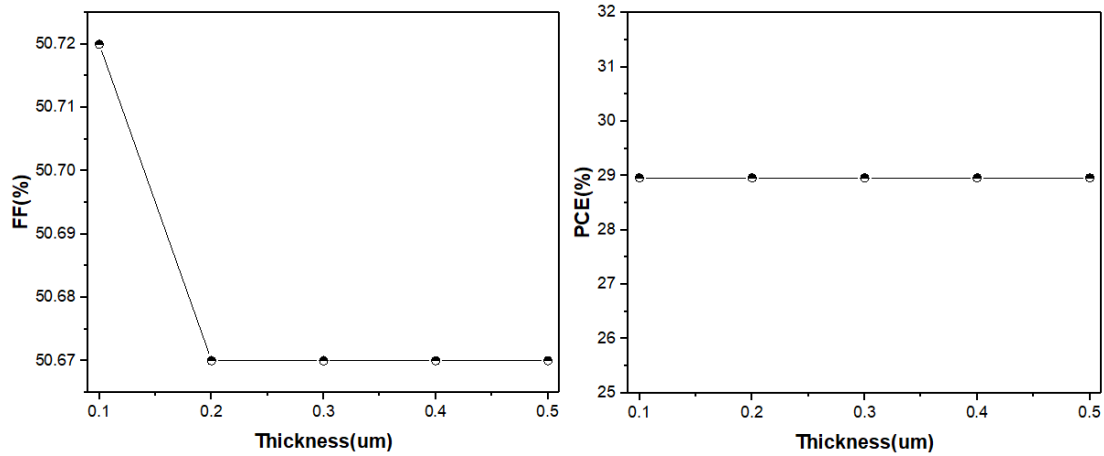


Figure III.12: Thickness effect of BSF layer on performance solar cell

III.5.2 Doping effect:

In figure III.12, the variation of defect density from $E18 \text{ cm}^{-3}$ to $E21 \text{ cm}^{-3}$ shows that J_{SC} a constant value for all the range of defect density (38.35 mA/cm^2), V_{OC} has a good value up to defect density of $E19 \text{ cm}^{-3}$, FF decrease till its lower value of 50.65% at a defect density of $E21 \text{ cm}^{-3}$ and the PCE each the 28.96 % at the maximum limit of doping.

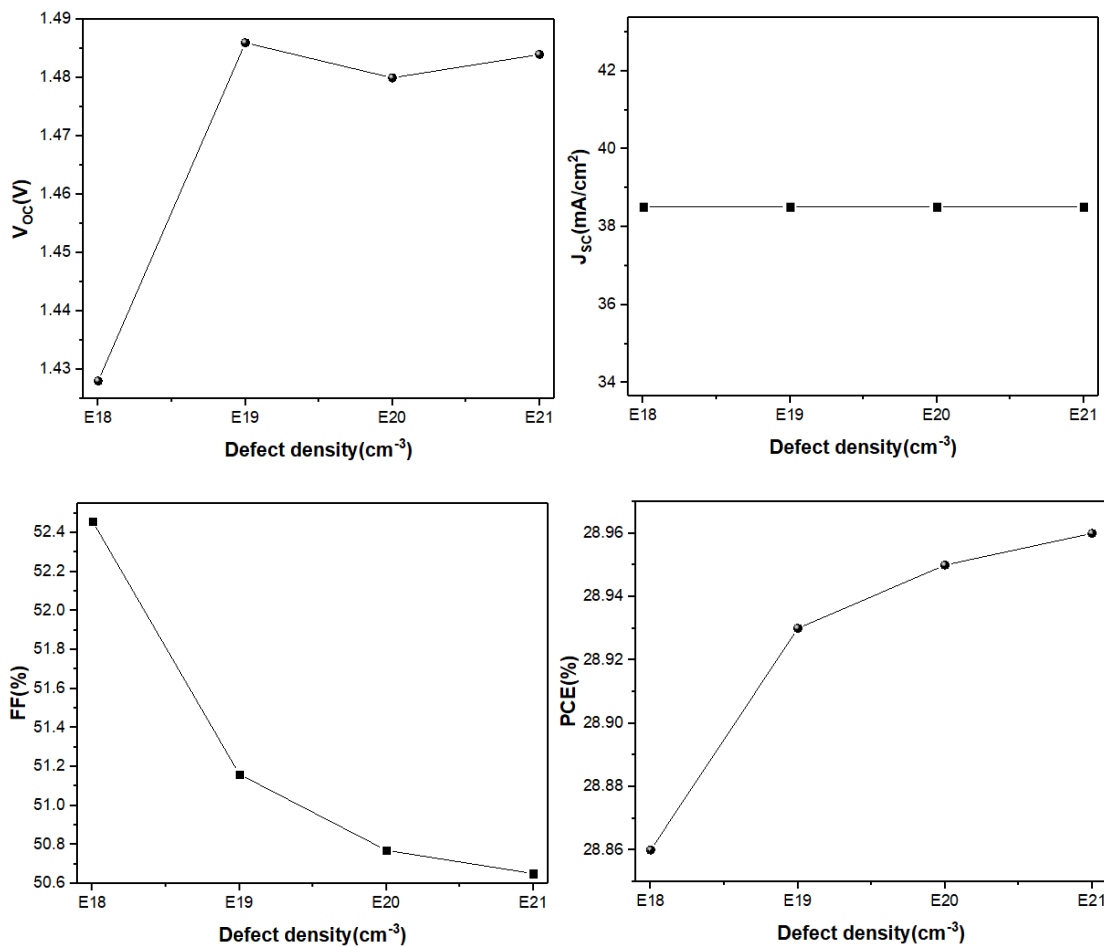


Figure III.13: Doping effect of BSF layer on performance solar cell

As conclusion, after the simulation, modeling and optimization, we found that our suggested model gives better results than the model of P. Roy et all [31], as illustrated bellow in table III.4

Structure	J_{sc} (mA/cm ²)	Voc(V)	FF (%)	PCE (%)
FTO/ZnO/ CsSn0.5Ge0.5I3/CuI/Au [31]	24.21	1.203	84.07	24.51
FTO/IGZO/CsSn0.5Ge0.5I3/ CsSnCI3/ CsSnCI3/CuO2/Au	38.4	1.486	52.48	28.96

Table III.4. Comparison between the conventional and the suggested model.

Conclusion:

In this work we studied via optimization all layers of the suggested structure according to the defect density and thickness. SCAPS-1D simulator gives the opportunity to study the geometrical, electrical and physical parameters, in the way of study their impact on the output performance. SCAPS simulator facilitate to know and select the adequate ETL and HTL via defect density and thickness, the perovskite materials are necessary in the structure configuration.

GENERAL

CONCLUSION

Among all third-generation solar cell photovoltaic technologies that have been researched over the last two decades, the only technology that significantly marked the energy conversion efficiency consists of solar cells based on structured materials based on perovskite, according to that, we first conducted a theoretical study on the principle working of solar cells, their electrical characteristics, the photovoltaic parameters, different used technologies and finally the PV solar cell based on the semiconductor materials such as the employed perovskite absorber. In this work we used the numerical simulation to study the characteristics of solar cell based on perovskite like: CsSn_{0.5}Ge_{0.5}I₃, CsSnCl₃ and CsSnCl₃. We also optimized physical, electrical and geometrical parameters to get the maximum of power conversion efficiency. The numerical modeling and simulation were done by the last version of the software SCAPS1D, to investigate the impact of thickness and doping of the inserted inputs, via using many ETL and HTL we arrive to locate the best inputs of the suggested structure in order to increase the PCE.

Our work based on the suggested configuration of solar cell and the optimization of all used parameters like thickness and defect density of ETL, HTL, absorber, number of layers, doping type, and front/back contacts...etc.

The proposed structure of triple gadded perovskite shows a good performance according the PCE of 28.96 %, $J_{SC}= 38.4 \text{ mA/cm}^2$, $V_{OC}=1.486 \text{ V}$ and $FF=52.48\%$.

BIBLIOGRAPHIC

REFERENCES

REFERENCES

- [1] : EL JOUAD, Zouhair. *Réalisation et caractérisation des cellules photovoltaïques organiques*. 2016. Thèse de doctorat. Angers.
- [2] : Krebs, F. C. "The development of organic and polymer photovoltaics." *Solar Energy Materials and Solar Cells* 83.2-3 (2004).
- [3] : ALEM-BOUDJEMLINE, Salima. *réalisation et caractérisation de cellules photovoltaïques plastiques*. 2004. Thèse de doctorat. Université d'Angers.
- [4] : Chodos, Allen. "April 25, 1954: Bell labs demonstrates the first practical silicon solar cell." *APS News-This month in Physics history* (2009).
- [5] : SLIMANI, Moulay Ahmed. *Cellules solaires pérovskites imprimées et optimisation des couches pérovskites pour les cellules tandems*. 2019. Thèse de doctorat. École de technologie supérieure.
- [6] : FAHRENBRUCH, Alan et BUBE, Richard. *Fundamentals of solar cells: photovoltaic solar energy conversion*. Elsevier, 2012.
- [7] : VERRIER, Claire. *Fabrication et caractérisation avancée de cellules photovoltaïques à base de nanofils de ZnO*. 2017. Thèse de doctorat. Université Grenoble Alpes.
- [8] : JÄGER, Klaus-Dieter, ISABELLA, Olindo, SMETS, Arno HM, *et al.* *Solar energy: fundamentals, technology and systems*. UIT Cambridge, 2016.
- [9] : AICHA, HAOUECHE et BOCHRA, MECHRI. *Etude et simulation d'une cellule solaire à pérovskite hybride à base de germanium par le simulateur SCAPSI-D*. 2021. Thèse de doctorat. Faculté des Sciences et Technologies.
- [10] : SOMIA, Mayouf. *Modélisation et simulation d'un système photovoltaïque connecté au réseau électrique avec une commande vectorielle*. 2016. Thèse de doctorat. UNIVERSITE DE MOHAMED BOUDIAF M'SILA FACULTE DE TECHNOLOGIE.
- [11] : HAJJAJI, A., JEMAI, S., TRABELSI, K., *et al.* Study of TiO₂ nanotubes decorated with PbS nanoparticles elaborated by pulsed laser deposition: Microstructural, optoelectronic and photoelectrochemical properties. *Journal of Materials Science: Materials in Electronics*, 2019, vol. 30, p. 20935-20946.
- [12] : I. w. s. o. P. P. G. Fraunhofer Institute for Solar Energy Systems, Fraunhofer ISE: Photovoltaics Report updated: 2021, 2021.
- [13] : POORTMANS, Jef et ARKHIPOV, Vladimir (ed.). *Thin film solar cells: fabrication, characterization and applications*. John Wiley & Sons, 2006.

- [14] : HADOUCHI, Warda. *Etude de l'utilisation du ZnO comme contact de type n dans des dispositifs photovoltaïques à base de pérovskite hybride*. 2017. Thèse de doctorat. Université Paris Saclay (COMUE).
- [15]: NREL,(2019). Best Research-Cell Efficiency Chart. Repéré à <https://www.nrel.gov/pv/cellefficiency.html>
- [16] : ANAYA, Miguel, LOZANO, Gabriel, CALVO, Mauricio E., *et al.* ABX₃ perovskites for tandem solar cells. *Joule*, 2017, vol. 1, no 4, p. 769-793.
- [17] : GHENO, Alexandre, VEDRAINE, Sylvain, RATIER, Bernard, *et al.* π -Conjugated materials as the hole-transporting layer in perovskite solar cells. *Metals*, 2016, vol. 6, no 1, p. 21.
- [18] : MERIEM, Goufi, BADR, Hamdouni, et MANEL, Bouhouche. *Etude et Simulation D'une Cellule Photovoltaïque à Pérovskite*. 2021.
- [19] : P. Edelman, W. Henley et J. Lagowski, « Imagerie de longueur de diffusion de photoluminescence et de porteurs minoritaires dans le silicium et le GaAs », *Semicond. Sci. Technol.*, Vol. 7, non. 1A, p. A22 – A26, janvier 1992.
- [20] : J.-W. Lee, D.-J. Seol, A.-N. Cho et N.-G. Park, « Pérovskite à haute efficacité cellules solaires basées sur le polymorphe noir de HC (NH₂) 2PbI₃, « *Advanced Matériaux*, vol. 26, non. 29, pages 4991 à 4998, 2014.
- [21] : V. Sarritzu et al., « Bande interdite directe ou indirecte dans les pérovskites aux halogénures de plomb hybrides ? », *Adv. Opter. Mater.*, Vol. 6, non. 10, p. 1701254, mai 2018.
- [22] : H. Zhou, Q. Chen, G. Li, S. Luo, T.b. Song, H.S. Duan, Z. Hong, J. You, Y. Liu and Y. Yang, “interface engineering of highly efficient perovskite solar cells”, *science*, 345 (2014) 542-546.
- [23] : Zhang, R.,Jiang, B. and CAO, W. elastic piezoelectric and dielectric properties of multidomain.0.67PB(Mg_{1/3}Nb_{2/3})O₃-0.33PbTiO₃ single crystals. *Journal of appliedPhysi c*, 90 (2001) 3471-3475.
- [24] : Q. Chen et al., « Sous le feu des projecteurs : la pérovskite hybride aux halogénures organiques et inorganiques pour les applications optoélectroniques », *Nano Today*, vol. 10, non. 3, p. 355-396, juin 2015.

- [25] : P. Edelman, W. Henley et J. Lagowski, « Imagerie de longueur de diffusion de photoluminescence et de porteurs minoritaires dans le silicium et le GaAs », *Semicond.Sci. Technol.*, Vol. 7, non. 1A, p. A22 – A26, janvier 1992.
- [26] : Chakrabarti T, Saha M, Khanda A, Sarkar SK. Modeling of Lead-Free CH₃NH₃SnI₃-Based Perovskite Solar Cell Using ZnO as ETL. *Advances in Communication, Devices and Networking*: Springer; 2018. p. 125-31.
- [27] : Calio L, Kazim S, Graetzel M, Ahmad S. Hole - matériaux de transport pour cellules solaires à pérovskite. *Angewandte Chemie édition internationale* 2016 ; 55 : 14522-45.
- [28] : Tress W, Marinova N, Inganäs O, Nazeeruddin MK, Zakeeruddin SM, Graetzel M. Le rôle de la couche de transport de trous dans les cellules solaires à pérovskite, réduisant la recombinaison et augmentant l'absorption. 2014 IEEE 40th Photovoltaic Specialist Conference (PVSC) : IEEE ; 2014. p. 1563-6.
- [29] : Zhang Y, Liu W, Tan F, Gu Y. Le rôle essentiel de la couche de transport de trous poly (3-hexylthiophène) dans les cellules solaires à pérovskite. *Journal des sources d'énergie* 2015 ; 274 : 1224-30.
- [30] : SCAPS Manuel ,18 MAI 2020
- [31]: SABBAB, Hussein. Numerical simulation of 30% efficient lead-free perovskite CsSnGeI₃-based solar cells. *Materials*, 2022, vol. 15, no 9, p. 3229.
- [32]: Roy, P., & Khare, A. (2021). Analysis of an efficient and eco-friendly CsGeSnI₃ based perovskite solar cell: A theoretical study. *Materials Today: Proceedings*, 44, 2997-3000.
- [33]: BHATTARAI, Sagar, PANDEY, Rahul, MADAN, Jaya, et al. A novel graded approach for improving the efficiency of Lead-Free perovskite solar cells. *Solar Energy*, 2022, vol. 244, p. 255-263.
- [34]: DAS, Abhijit, SAMAJDAR, Dip Prakash, et RAVIDAS, Babban Kumar. Investigation of the Efficiency of CsGeI₃-based solar cell using SCAPS-1D modeling and simulation. In : 2022 IEEE International Conference of Electron Devices Society Kolkata Chapter (EDKCON). IEEE, 2022. p. 91-95.